

UNCLASSIFIED

AD NUMBER
AD801906
NEW LIMITATION CHANGE
TO Approved for public release, distribution unlimited
FROM Distribution authorized to U.S. Gov't. agencies and their contractors; Critical Technology; NOV 1966. Other requests shall be referred to Arnold Engineering Development Center, Attn: AETS, Arnold AFS, TN.
AUTHORITY
USAEDC ltr, 23 Jan 1975

THIS PAGE IS UNCLASSIFIED

**AEDC-TR-66-197**



**THE VON KÁRMÁN GAS DYNAMICS FACILITY  
1000-FT HYPERVELOCITY RANGE**

**DESCRIPTION, CAPABILITIES, AND  
EARLY TEST RESULTS**

**Compiled by  
P. L. Clemens  
ARO, Inc.**

**November 1966**

This document is subject to special export controls and each transmittal to foreign governments or foreign nationals may be made only with prior approval of Arnold Engineering Development Center (AEDC), Arnold AF Station, Tennessee.

**VON KÁRMÁN GAS DYNAMICS FACILITY  
ARNOLD ENGINEERING DEVELOPMENT CENTER  
AIR FORCE SYSTEMS COMMAND  
ARNOLD AIR FORCE STATION, TENNESSEE**

**Best Available Copy**

801906

# ***NOTICES***

When U. S. Government drawings specifications, or other data are used for any purpose other than a definitely related Government procurement operation, the Government thereby incurs no responsibility nor any obligation whatsoever, and the fact that the Government may have formulated, furnished, or in any way supplied the said drawings, specifications, or other data, is not to be regarded by implication or otherwise, or in any manner licensing the holder or any other person or corporation, or conveying any rights or permission to manufacture, use, or sell any patented invention that may in any way be related thereto.

Qualified users may obtain copies of this report from the Defense Documentation Center.

References to named commercial products in this report are not to be considered in any sense as an endorsement of the product by the United States Air Force or the Government.

THE VON KÁRMÁN GAS DYNAMICS FACILITY  
1000-FT HYPERVELOCITY RANGE

---

DESCRIPTION, CAPABILITIES, AND  
EARLY TEST RESULTS

Compiled by

P. L. Clemens  
ARO, Inc.

This document is subject to special export controls and each transmittal to foreign governments or foreign nationals may be made only with prior approval of Arnold Engineering Development Center (AEDC), Arnold AF Station, Tennessee.

### FOREWORD

The work reported herein was sponsored by the Arnold Engineering Development Center (AEDC), Air Force Systems Command (AFSC). The report was prepared by ARO, Inc. (a subsidiary of Sverdrup & Parcel and Associates, Inc.), contract operator of the AEDC under Contract AF40(600)-1200. The ARO Project No. was VG2706. The manuscript was submitted for publication on September 14, 1966.

The editor wishes to express sincere appreciation to J. L. Potter, Manager of the VKF Aerophysics Branch, for very helpful guidance given during the assembly of the information contained in this report. Thanks are also due to the VKF Aerophysics Branch staff members whose work is described here. (Papers more fully covering their work will be found listed among the References cited in this report.)

This technical report has been reviewed and is approved.

Donald E. Beitsch  
Major, USAF  
AF Representative, VKF  
Directorate of Test

Leonard T. Glaser  
Colonel, USAF  
Director of Test

## ABSTRACT

The von Kármán Gas Dynamics Facility (VKF) 1000-ft Hypervelocity Range facility at the Arnold Engineering Development Center is described, and its current operating capabilities are presented. A brief sampling of test results obtained during early operation of the range is presented as well. Among these are: (1) results of sphere drag measurements over the Reynolds number range  $3 \leq Re_2 \leq 10^6$ ; (2) results of the measurements of flow transition locations and wake velocities behind spheres, as obtained through the use of a 35-GHz Doppler radar system; (3) results of measurements of electron densities in the wakes of spheres, as obtained using r-f cavity and microwave techniques; (4) results of the measurement of radiation from the shock caps of spheres; and (5) results of the effect of unit Reynolds number on the location of flow transition in the wakes of cones, as measured using a high sensitivity schlieren system. In each case, the data results presented are correlated with measurements made at other establishments or with data based on available theory. The correlations are shown to be generally reasonable. An appendix describes the VKF 100-ft Hypervelocity Range K, which served as a pilot facility during the development of the 1000-ft range and which continues in service.

## CONTENTS

	<u>Page</u>
ABSTRACT . . . . .	iii
I. INTRODUCTION . . . . .	1
II. 1000-FT HYPERVELOCITY RANGE DESCRIPTION . . . . .	1
III. LAUNCHER PERFORMANCE . . . . .	2
IV. RANGE INSTRUMENTATION	
4.1 Pressure . . . . .	3
4.2 Temperatures . . . . .	3
4.3 Shadowgraphs . . . . .	3
4.4 Schlieren Photography . . . . .	4
4.5 Microwave and R-F Cavity Measurements . . . . .	4
4.6 Radiometric and Spectrographic Measurements . . . . .	5
4.7 High-Speed Photography . . . . .	5
4.8 Recording Equipment . . . . .	6
V. TYPICAL TEST RESULTS	
5.1 Sphere Drag Measurements . . . . .	6
5.2 Wake Velocity Measurements . . . . .	7
5.3 Transition from Laminar to Turbulent Flow in Sphere Wakes . . . . .	7
5.4 Wake Electron Density Measurements . . . . .	7
5.5 Shock Cap Radiation Measurements . . . . .	8
5.6 Unit Reynolds Number Effect on Transition in Wakes of Cones . . . . .	9
REFERENCES . . . . .	9
APPENDIX -- VKF 100-FT HYPERVELOCITY RANGE K. . . . .	12

## ILLUSTRATIONS

Figure

1. VKF 1000-ft Hypervelocity Range G. . . . .	17
2. Launcher - VKF 1000-ft Hypervelocity Range G. . . . .	18
3. Distance Traveled before Nose Reached Melting Temperature . . . . .	19
4. Routine Data Flow - VKF 1000-ft Hypervelocity Range G. . . . .	20
5. Shadowgraph Configuration - VKF 1000-ft Hypervelocity Range G. . . . .	21

<u>Figure</u>	<u>Page</u>
6. Uprange View within VKF 1000-ft Hypervelocity Range G, Showing Shadowgraph Fresnel Lenses. . .	22
7. Shadowgram - VKF 1000-ft Hypervelocity Range G. . . . .	23
8. X-Ray Shadowgram - VKF 1000-ft Hypervelocity Range G. . . . .	24
9a. Single-Frame Schlieren Photograph - VKF 1000-ft Hypervelocity Range G. . . . .	25
9b. Turbulent Wake behind a Hypervelocity Sphere . . . . .	26
9c. Inviscid Wake behind a Hypervelocity Sphere. . .	27
10a. Instrumentation Equipment - VKF 1000-ft Hypervelocity Range G. . . . .	29
10b. Exterior View - VKF 1000-ft Hypervelocity Range Instrumentation Equipment. . . . .	31
10c. Resonant R-F Cavity and Focused Microwave Probes - Uprange View. . . . .	32
11. Variation of Support-Free Sphere Drag Coefficient with Reynolds Number ( $8 < M_{\infty} < 15$ ). . . . .	33
12. 35-GHz Oblique Doppler Radar Signals	
a. Nonablating Model. . . . .	34
b. Ablating Model . . . . .	34
13. Wake Velocity behind a Sphere. . . . .	35
14. Comparison of Schlieren and Microwave Measurements of Inner Wake Transition Distance . . . . .	36
15. Electron Density Decay in Wakes of Nonablating Spheres. . . . .	37
16. Comparison of Calculated Forcing and Measured Response of Narrow-Slit Radiometer . . . . .	38
17. Measurements of Total Radiance of Equilibrium Shock Cap of Sphere. . . . .	39
18. Transition Reynolds Number Variation with Body Reynolds Number. . . . .	40

## SECTION I

### INTRODUCTION

The Aerophysics Branch of the von Kármán Gas Dynamics Facility (VKF) operates an array of aerophysical laboratory testing facilities which includes two hypervelocity impact ranges, a low-density wind tunnel, and two evacuable hypervelocity ranges having test chamber lengths of 100 and 1000 ft. The primary purpose of this report is to describe the capabilities of the VKF 1000-ft Hypervelocity Range G and to present a sampling of test results obtained during its early operation. However, brief mention of the other test units is in order.

The VKF Tunnel L is a continuous-type, arc-heated, low-density wind tunnel which offers a unique capability for gas dynamic studies at simulated altitudes between 50 and 60 miles. Axisymmetric nozzles are used having throat diameters of 0.1 to 1.2 in. and exits of 2.0 to 8.2 in. (Three, contoured nozzles are available, and their use results in the absence of flow gradients in the test section.) The tunnel operates at Mach numbers between 4 and 16 and at Reynolds numbers between 300 and 3500 per in.

The Hypervelocity Impact Ranges S-1 and S-2 are used primarily in evaluations of the structural and radiation observable effects which occur as a result of collisions between projectiles and simulated spacecraft or warhead structures. They are outfitted with two-stage, light-gas guns of 0.5-in. bore which are capable of launching 0.7-gm projectiles at velocities as great as 32,000 ft/sec.

The 100-ft Hypervelocity Range K served initially as a pilot facility for the later 1000-ft range and now engages in other test work. A complete description of the 100-ft range appears as the Appendix to this report.

## SECTION II

### 1000-FT HYPERVELOCITY RANGE DESCRIPTION

The VKF 1000-ft Hypervelocity Range G, a free-flight test unit, appears in Fig. 1. The range is equipped with a test model launcher of 2.5-in. bore diameter. This launcher, shown in Fig. 2, is a two-stage, powder-hydrogen gun approximately 100 ft long. The range is a 1000-ft-long, 10-ft-diam, black steel tube which is wholly contained within an underground service tunnel 20 ft wide and 14 ft high. A blast

chamber which absorbs the expanding muzzle gases makes up the initial 85 ft of the range, and it is in this chamber that the test model is separated from the sabot which adapts it to the bore of the launcher. A guillotine valve, having a closing time of approximately 10 msec, separates the blast chamber from the remainder of the range. Major dimensions of both the range and the launcher appear in Table I, where numbers and locations of stations at which the more routine measurements are made are also found. A three-stage system of mechanical vacuum pumps provides the air pressure desired within the range. Pressure can be adjusted to any value between atmospheric and  $20\text{-}\mu\text{Hg}$ . The pumpdown time required to produce a range pressure level of 15-mm Hg is approximately one hour; to the  $20\text{-}\mu\text{Hg}$  level, it is approximately 2-3/4 hr. Range temperature is regulated at a level of  $75^{\circ}\text{F}$ ,  $\pm 1^{\circ}\text{F}$ . The range can be operated at a test rate of one to two shots per 8-hr day, depending upon the complexity of the test program.

### SECTION III LAUNCHER PERFORMANCE

Table II indicates typical limits of performance for the 2.5-in.-diam launcher which were current in September 1966. Other model configurations than those indicated can be launched. Launcher performance is the subject of a continuing evaluation and development program in the VKF. Reference 1 describes work directed toward optimizing the performance of two-stage, light-gas launchers and presents typical results. Reference 2 reports methods of microwave reflectometry applied in the empirical evaluation of launcher performance.

It must be recognized that over a large portion of the velocity-pressure capability of the range, and for many model shapes, ablation of many model materials can be expected to commence during flight. Figure 3 presents the results of computations which indicate the nature and extent of the ablation problem for a number of typical cases.

### SECTION IV RANGE INSTRUMENTATION

A diagram showing data flow and readout equipment for the more routine measurements in the 1000-ft Hypervelocity Range G appears as Fig. 4.

#### 4.1 PRESSURE

Pressures are monitored continuously at three gaging stations along the length of the range. Precision, variable-capacitance transducers with remote potentiometer readout are used. Measurement errors using this system, over the span from atmospheric pressure to 1-mm Hg, do not exceed 1 percent of reading; 2-percent error limits are judged to apply from 1-mm to 40- $\mu$  Hg, based on comparisons with separate means of measurement which serve as secondary standards at pressures above 1-mm Hg. Ionization and McLeod gages are used at pressures below 40- $\mu$  Hg. The measurement system reference vacuum is maintained at less than 0.01- $\mu$  Hg and is monitored with an ionization gage.

#### 4.2 TEMPERATURES

Range temperatures are monitored continuously at three gaging stations. Copper-constantan thermocouples are used in making the temperature measurements, and a multipoint, strip-chart servo-potentiometer provides their readout. Overall error limits are  $\pm 1.0^{\circ}\text{F}$ . Dew-point temperatures over the span  $-50^{\circ}\text{F}$  to  $+100^{\circ}\text{F}$  are also measured at three stations. Transducers which take advantage of the unique hygroscopic-conductivity properties of lithium chloride are used. Readout is remote, and errors in the dew-point measurements do not exceed  $\pm 1.5^{\circ}\text{F}$  limits.

#### 4.3 SHADOWGRAPHS

Forty-three, dual-axis, spark shadowgraphs (Ref. 3), as shown in Fig. 5, are situated at 20-ft intervals along the range. Optical axes at each shadowgraph station are mutually orthogonal with the range centerline. Viewfield diameter of each shadowgraph is 30 in., measured at the range centerline. Exposure duration provided by the spark light sources is 0.12  $\mu\text{sec}$ . Large Fresnel lenses (Fig. 6) serve as intensifying screens for the shadowgraphs. The Fresnel lenses bear scribed fiducial grids, and the shadowgraphs are designed primarily to produce data describing time-resolved projectile positions and attitudes rather than flow information. A typical shadowgram appears as Fig. 7. A digitized film reader is used to carry out numerical interpretations of the shadowgrams, and these are used to provide position-attitude time histories which are fitted to a computer program from which aerodynamic coefficients evolve. Timing information, which makes this possible, is accumulated in a multi-channel digital event chronograph. This instrument accumulates time-

resolved annunciations of projectile arrival at any 59 measurement stations, stores the information during projectile flight, and presents it in tabulated form, immediately following the shot, with each time entry numerically identified with the event it describes. Event timing resolution is  $\pm 0.1$   $\mu$ sec using this system. X-ray shadowgraphs of 0.1- $\mu$ sec exposure duration record early projectile positions and attitudes in the blast chamber, where bright muzzle flash precludes the use of ordinary visible light systems. These X-ray systems also enable structural examinations of models in the blast chamber and in later flight. A typical X-ray shadowgram appears as Fig. 8; serrated sabot segments are seen separating from the projectile.

#### 4.4 SCHLIEREN PHOTOGRAPHY

A high-sensitivity, single-pass, schlieren photographic system is positioned 88.5 ft from the range entrance to provide photographic recording of flow information. The schlieren system has a viewfield diameter of 30 in. and is operable in either single-frame or multi-frame modes. In the latter, as many as 20 frames are obtained. Exposure duration is 0.1  $\mu$ sec. Examples of schlieren photography using this system appear as Figs. 9a, b, and c.

#### 4.5 MICROWAVE AND R-F CAVITY MEASUREMENTS

In work relating to wake diagnostics, additional instrumentation systems are used. These appear in Fig. 10. A resonant r-f cavity is situated near the range entrance and is used in making measurements of effective electron line density. The ranges of effective electron densities over which the r-f cavity, and a following array of microwave diagnostic equipment, provide measurements are listed in Table III. Two, dual-channel, focused, phase-quadrature, microwave interferometers are operated at each of two frequencies (35 and 70 GHz). Microwave transmission and reflection properties of wakes are measured using five broadside probing systems operating over a full four octaves of frequency. The axial locations within projectile wakes at which effective cutoff electron densities are realized (see Table III) can be determined using these systems. An oblique Doppler radar system operating at a frequency of 35 GHz is also provided and is equipped with auxiliary parasite and transmitted-signal sensing antennas. The Doppler radar signal serves as a measure of the velocity of reflective media within projectile wakes. The parasite antenna enables observation of the specular character of wakes illuminated by the beam of microwave energy, while the transmitted-signal antenna provides

additional information on wake transparency. The viewfield dimensions of the microwave systems, as measured along the range centerline between the -10-db points, are listed in Table III. The microwave systems operate with signal-to-noise ratios of, typically, 30 db.

#### 4.6 RADIOMETRIC AND SPECTROGRAPHIC MEASUREMENTS

Flow field studies in the range are also supported by a battery of photomultiplier radiometers (Ref. 4) and spectrographic equipment shown in Fig. 10. Spectral characteristics of the radiometers available are outlined in Table IV, and the radiometers themselves are interchangeable among the locations indicated in Fig. 10. Radiometer viewfields, as measured along the range centerline, are adjustable over broad limits to a minimum of one millimeter. In response to step-function forcing, the radiometers and their readout oscilloscopes operate with rise times of 14 nanoseconds (10 to 90 percent of total excursion) and accurately reproduce nominal square wave input signals having durations of 0.5  $\mu$ sec to 2 msec. The radiometers have absolute intensity calibrations traceable to the National Bureau of Standards.

The complement of spectrographs with which the range is outfitted is described in Table V. As with the radiometers, viewfields of the spectrographs can be confined to a dimension as small as one millimeter along the range centerline. In general, only time-integrated spectra are photographically recorded. However, one of the 3/4-m grating spectrographs is equipped with a group of six photomultipliers to enable time-resolved readout of radiant energy intensities at selected wavelengths. Of these six photomultipliers, two accommodate 5- $\text{\AA}$  bandwidths. The remaining four are positioned to accommodate bandwidths of 100  $\text{\AA}$  on either side of each of these two 5- $\text{\AA}$  bands. Use of the photomultipliers does not interfere with the normal functioning of the spectrograph in recording spectra on film.

#### 4.7 HIGH-SPEED PHOTOGRAPHY

As indicated in Fig. 10, an image converter camera is available for use in photographing the luminous flow fields enshrouding projectiles during their flights through the range. Viewfield dimensions provided by this camera at the range centerline are 4 in. (along the flight axis) by 3 in. The camera will produce from one to three frames and is operable with exposure durations of 50, 100, and 200 nsec per frame. The inter-frame interval is adjustable in steps to

values of 0.5, 1.0, 2.0, 5.0, and 10  $\mu$ sec. In addition, several high-speed cine cameras, operating at maximum frame rates of about 7000 per second, are provided and can be used at any of a large number of range stations. (One is indicated in Fig. 10.) These cameras can be used to record flight of the projectile over a large portion of its trajectory.

#### 4.8 RECORDING EQUIPMENT

A 36-channel oscillograph and a group of oscilloscopes (frequency response: d-c to 50 MHz) serve the range, as does a 14-channel magnetic tape system (frequency response: d-c to 40 KHz,  $\pm 1$  db/f-m mode; 300 Hz to 500 KHz,  $\pm 3$  db/direct mode).

### SECTION V TYPICAL TEST RESULTS

The test results described here are representative of some obtained during very early aeroballistic range work performed in the 1000-ft Hypervelocity Range of the von Kármán Gas Dynamics Facility and in its 100-ft pilot facility which is described in the Appendix. These results should not be construed to represent ultimate test capabilities.

#### 5.1 SPHERE DRAG MEASUREMENTS

Drag coefficients of spheres have been measured in VKF range work with an accuracy of  $\pm 1.5$  percent for  $Re_2 > 10^4$  and over the velocity range from 3,000 to 21,000 ft/sec. ( $Re_2$  = Reynolds number based on flow conditions just behind shock, and sphere diameter.) Techniques for constructing and for launching models made of very low density materials (approaching one pound per cubic ft) have been developed and have enabled further measurement of sphere drag coefficients with an accuracy of  $\pm 4$  percent for  $3 \leq Re_2 \leq 10^6$  and over the velocity range from 3,000 to 12,000 ft/sec. Complete results of this work have been reported by Bailey in Ref. 5, where it is shown that this wide range of test conditions has made it possible to study the initial departure of sphere drag coefficient from the high Reynolds number continuum level and also to make measurements at free-stream Knudsen numbers approaching unity. The results, as presented in Ref. 5, are summarized in Fig. 11, where it is evident that at the low Reynolds numbers, they are consistent with results obtained in other low-density, hypersonic test facilities (Refs. 6, 7, and 8). Values of drag coefficient predicted by the theoretical work of Davis and Flugge-Lotz (Ref. 9) also appear in Fig. 11.

## 5.2 WAKE VELOCITY MEASUREMENTS

A 35-GHz oblique Doppler radar system, as shown in Fig. 10, has been used to measure the velocities of reflecting media contained within the wakes of hypervelocity spheres. Spheres of a variety of materials having wide ranges of densities and melting temperatures have been used in this work. Doppler radar velocity measurements in sphere wakes were obtained only in those cases wherein ablation of the model occurred. Figures 12a and b show typical Doppler radar return signals from, respectively, a nonablating model, and an ablating model and its wake. Doppler radar wake velocity measurements made for the ablating cases are in good agreement with one another and correlate well with data gathered using nearly identical instrumentation at the General Motors Defense Research Laboratories (Ref. 10). The VKF test results and data correlations are described in detail in Ref. 11 and appear summarized in Fig. 13, where wake velocity measurements made by other techniques and also at other establishments (Refs. 12 and 13), as well as theoretical data (Ref. 14), are plotted for comparison. Since no Doppler radar reflections have been observed from the wakes of nonablating models in the VKF, the results of this work suggest that the products of ablation serve as the reflecting media and that they do not radically alter the structure of the fluid dynamic wake.

## 5.3 TRANSITION FROM LAMINAR TO TURBULENT FLOW IN SPHERE WAKES

The 35-GHz Doppler radar system has also enabled measurements of the point at which inner wake transition occurs in sphere wakes. Data typical of these measurements appear in Fig. 14, where transition measurements from another source (Ref. 15), made using a similar system, are shown for comparison. Also indicated is a band representing inner wake transition measurements made using schlieren photography during a large number of test shots in the VKF (Ref. 11). Qualitative agreement among data from the three sources is evident.

## 5.4 WAKE ELECTRON DENSITY MEASUREMENTS

A group of data points plotted in Fig. 15 represents measurements of electron density made in the VKF in the wakes of nonablating, 0.5-in.-diam solid copper spheres. The majority of the VKF electron density measurements in Fig. 15 were made using the resonant r-f cavity shown in Fig. 10 and whose characteristics are outlined in Table III. As was indicated in Section 4.5, the resonant cavity provides a measure of effective electron line density. In preparing

Fig. 15, measurements of electron line density made using the cavity were converted to values of true electron density by assuming the electron wake diameter to be the same as that of the visible wake, as given in Ref. 11. In Fig. 15, the VKF cavity measurement results for sphere velocities of about 18,000 ft/sec are seen to compare favorably with results obtained by the MIT Lincoln Laboratory (Ref. 16) where a similar resonant cavity was used for measurements at nearly equal velocities.

Also shown in Fig. 15 are limited data, obtained in this same range of velocities, using the 4.25-GHz broadside microwave probes which were discussed in Section 4.5. These results fall near measurements made by the General Motors Defense Research Laboratories (Ref. 17), again at velocities near 18,000 ft/sec. The latter data (Ref. 17) were obtained using focused microwave interferometers.

Additional data obtained at higher sphere velocities (near 21,000 ft/sec) also appear in Fig. 15. The VKF measurements at these velocities were obtained using broadside probes and can be compared with the General Motors Defense Research Laboratories focused microwave interferometer measurements, drawn from Ref. 17. Correlation between the data obtained at the two establishments at these higher velocities, and using the differing methods of measurement, appears to be quite good.

## 5.5 SHOCK CAP RADIATION MEASUREMENTS

The photomultiplier radiometers shown in Figs. 10a and b and described in Table IV have been used to measure the radiant energy from the shock caps of spherical models. During the evaluations of these radiometers (Ref. 4), the forms of forcing functions representing shock cap radiance were analytically derived for radiometer slit widths corresponding to various viewfield dimensions, measured along the flight path. (These calculated forcing functions were based on the radiance per unit length in the shock cap of a 3/8-in.-diam sphere, traveling at 16,000 ft/sec, through air at a pressure of 76-mm Hg.) In Fig. 16, the calculated forcing functions are plotted together with corresponding, normalized radiometer data recorded during three test shots. (In constructing Fig. 16, the maximum value of the radiance forcing function calculated for the 6.4-mm slit was adjusted to equal the peak value of the corresponding measured radiant intensity data; all other forcing functions were adjusted in the same ratio as was the one for the 6.4-mm slit.) The close agreement between the form of the computed curves and the recorded empirical data lends credence to the analytical method used in

deriving the forcing functions and also provides assurance that the response of the photomultiplier radiometers and their readout equipment is adequate to the making of measurements under these circumstances of testing.

Measurements of absolute shock cap radiant intensity for a number of shots are shown in Fig. 17. Here, the total shock cap radiance values, as measured by a single, broadband radiometer (S-5 spectral response -- Table IV), are shown as are the integrated values resulting from measurements made by ten narrow-band radiometers. A plot representing the theory of Gilmore (Ref. 18) also appears.

#### 5.6 UNIT REYNOLDS NUMBER EFFECT ON TRANSITION IN WAKES OF CONES

Experiments have been conducted in VKF range work to study the effects of ambient pressure, model size, cone semi-angle, and velocity upon the distance to transition in the wakes of slender, sharp cones. Schlieren photography, of which Fig. 9a is representative, was used in the making of the transition measurements. The work has been reported by Bailey in Ref. 19, and results are summarized in Fig. 18 where it is seen that for cones of both 5- and 10-deg semi-angle, transition Reynolds number decreases with decreasing unit Reynolds number. As Fig. 18 also demonstrates, aeroballistic range data obtained elsewhere (Ref. 20) for 12.5-deg semi-angle cones and wind tunnel data representing transition on the surface of 10-deg semi-angle cones (Ref. 21) behave similarly.

#### REFERENCES

1. Cable, A. J., DeWitt, J. R., and Prince, M. D. "Launcher Optimization Studies." AEDC-TR-65-204 (AD 471849), October 1965.
2. Hendrix, R. E. "Microwave Reflectometry in Interior Ballistics." AEDC-TR-66-54 (AD 482754), May 1966.
3. Clemens, P. L. and Hendrix, R. E. "Development of Instrumentation for the VKF 1000-ft Hypervelocity Range." Proceedings of the Second Symposium on Hypervelocity Techniques, University of Denver, March 1962.
4. Ball, H. W., Harris, H. G., and Hiatt, J. "Design and Evaluation of a Radiometer Circuit for Measuring Absolute Radiation from the Flow Field of a Hypervelocity

Projectile." Proceedings of the IEEE 2nd International Congress on Instrumentation in Aerospace Simulation Facilities, Stanford University, August 1966.

5. Bailey, A. B. "Sphere Drag Measurements in an Aerobal-  
listics Range at High Velocities and Low Reynolds Num-  
bers." AEDC-TR-66-59 (AD 633278), May 1966.
6. Kinslow, Max and Potter, J. L. "The Drag of Spheres in  
Rarefied Hypersonic Flow." AEDC-TDR-62-205 (AD 290519),  
December 1962.
7. Slattery, J. C., Friichtenicht, J. F., and Hamermesh, B.  
"Interaction of Micrometeorites with Gaseous Targets."  
AIAA Journal, Vol. 2, No. 3, March 1964, pp. 543-548.
8. Geiger, R. E. "Some Sphere Drag Measurements in Low-  
Density Shock Tunnel Flows." General Electric Report  
R63SD23, July 1963.
9. Davis, R. T. and Flugge-Lotz, I. "Second-Order Boundary-  
Layer Effects in Hypersonic Flow Past Axisymmetric  
Blunt Bodies." Journal Fluid Mechanics, Vol. 20,  
Part 4, 1964, pp. 593-623.
10. Primich, R. and Steinberg, M. "A Broad Survey of Free-  
Flight Range Measurements from the Flow about Spheres  
and Cones." GM Defense Research Laboratories TR 63-  
224, September 1963.
11. Bailey, A. B. "Turbulent Wake and Shock Shape of Hyper-  
velocity Spheres." AEDC-TR-66-32 (AD 484821), July  
1966.
12. Slattery, R. E. and Clay, W. G. "The Turbulent Wake of  
Hypersonic Bodies." American Rocket Society 17th An-  
nual Meeting and Space Flight Exposition, November 13-  
18, 1962, No. 2673-62.
13. Hidalgo, H., Taylor, R. L., and Keck, J. C. "Transition  
in the Viscous Wake of Blunt-Bodies at Hypersonic  
Speeds." Avco-Everett Research Laboratory Research  
Report 133, April 1961.
14. Lees, Lester and Hromas, Leslie. "Turbulent Diffusion  
in the Wake of a Blunt-Nosed Body at Hypersonic Speeds."  
Journal of the Aerospace Sciences, Vol. 29, No. 6,  
August 1962, pp. 976-993.
15. Primich, R. L., Robillard, P. E., Eschenroeder, A. Q.,  
Wilson, L., and Zivanovic, S. "Radar Scattering from

- Wakes." GM Defense Research Laboratories TR 65-01E, March 1965.
16. Kornegay, W. M. "Decay of Electron Density in the Wakes of Hypervelocity Spheres." Massachusetts Institute of Technology MIT-TR-370 (AD 612152), December 1964.
  17. Eschenroeder, A. Q., Hayami, R. A., Primich, R. I., and Chen, T. "Ionization in the Near Wakes of Spheres in Hypervelocity Flight." AIAA Paper No. 66-55, January 1966.
  18. Gilmore, F. R. "Approximate Radiation Properties of Air between 2000 and 8000°K." The Rand Corporation (Santa Monica, California) RM-3997-ARPA, March 1964.
  19. Bailey, A. B. "The Effect of the Unit Reynolds Number on Transition in the Wake of High Speed Sharp Slender Cones." AEDC-TR-66-137, July 1966.
  20. Slattery, R. E. and Clay, W. G. "The Turbulent Wake of Hypersonic Bodies." American Rocket Society 17th Annual Meeting and Space Flight Exposition, November 13-18, 1962, No. 2673-62.
  21. Potter, J. Leith and Whitfield, Jack D. "Recent Developments in Boundary Layer Research." AGARDograph 97, Part III, May 1965.

## APPENDIX

### VKF 100-FT HYPERVELOCITY RANGE K

#### RANGE DESCRIPTION

The VKF 100-ft Hypervelocity Range K, a free-flight test unit, appears in Fig. I-1. Test model launchers having bore diameters of 0.5, 0.625, 1.0, and 2.5 in. serve the range. All are powder-hydrogen launchers, and the three smaller units operate in two-stage configuration, while the largest is a single-stage gun. The test range is a 100-ft-long, 6-ft-diam, black steel tube which is wholly contained in a service building above grade. A 14-ft-long, 6-ft-diam blast chamber, which absorbs the expanding muzzle gases, joins the launcher to the range, and it is in this chamber that the test model is separated from the sabot which adapts it to the bore of the launcher. Major range and launcher dimensions appear in Table I-1, where numbers and locations of measurement stations also are found. A three-stage vacuum pumping system provides the air pressure desired within the range. Pressure can be adjusted to any value between atmospheric and 1.0- $\mu$ Hg.

#### RANGE INSTRUMENTATION

A diagram showing data flow and readout equipment for the 100-ft Hypervelocity Range K appears as Fig. I-2.

##### Pressure

Range pressure is monitored continuously using a precision, variable-capacitance transducer with potentiometer readout. Measurement errors using this system, over the span from atmospheric pressure to 1-mm Hg, do not exceed 1 percent of reading; 2-percent error limits are judged to apply from 1-mm to 40- $\mu$ Hg, based on comparisons with separate means of measurement which serve as secondary standards at pressures above 1-mm Hg. Ionization and McLeod gages are used at pressures below 40- $\mu$ Hg. The measurement system reference vacuum is maintained at less than 0.01- $\mu$ Hg and is monitored with an ionization gage.

##### Temperature

Range temperatures are monitored continuously at six gaging stations. Copper-constantan thermocouples are used in making the temperature measurements, and a multipoint, strip-chart servopotentiometer provides their readout. Overall error limits are  $\pm 1.0^\circ\text{F}$ .

### Shadowgraphs

Six, dual-axis, spark shadowgraphs are situated at 15-ft intervals along the range. Optical axes at each shadowgraph station are mutually orthogonal with the range centerline. Viewfield diameter of each shadowgraph is 12 in., measured at the range centerline. Exposure duration provided by the spark light source is 0.12  $\mu$ sec. Fresnel lenses serve as intensifying screens for the shadowgraphs, which are designed primarily to produce data describing projectile positions and attitudes rather than flow information. Time durations which separate the shadowgraph exposures are measured either by 10-MHz chronographs or by a multi-channel, digital event chronograph. In either case, event timing resolution is  $\pm 0.1$   $\mu$ sec. X-ray shadowgraphs of 0.1- $\mu$ sec exposure duration record early projectile positions and attitudes in the blast chamber, where bright muzzle flash precludes the use of ordinary visible light systems. These X-ray systems also enable structural examinations of models in the blast chamber in later flight.

### Schlieren Photography

A high-sensitivity, single-pass schlieren photographic system is positioned 15 ft from the range entrance to provide photographic recording of flow information. The schlieren system has a viewfield diameter of 12 in. and is operable in either single-frame or multi-frame modes. In the latter, as many as 20 frames are obtained. Exposure duration is 0.1  $\mu$ sec.

### Microwave and Radiometric Measurements

In work relating to flow field diagnostics, several additional instrumentation systems are used. Focused microwave systems, operating at frequencies of 10, 17, 35, and 70 GHz, function either as phase-shift or attenuation bridges. Time-resolving photomultiplier radiometers, with or without narrow band filters, measure radiation observables over the range of wavelengths from 2,000 to 10,000 Å. These radiometers have absolute calibrations traceable to the National Bureau of Standards.

### Recording Equipment

A 50-channel oscillograph and a group of oscilloscopes (frequency response: d-c to 50 MHz) serve the range, as does a 14-channel magnetic tape system (frequency response: d-c to 40 KHz,  $\pm 1$  db/f-m mode; 300 Hz to 500 KHz,  $\pm 3$  db/direct mode).

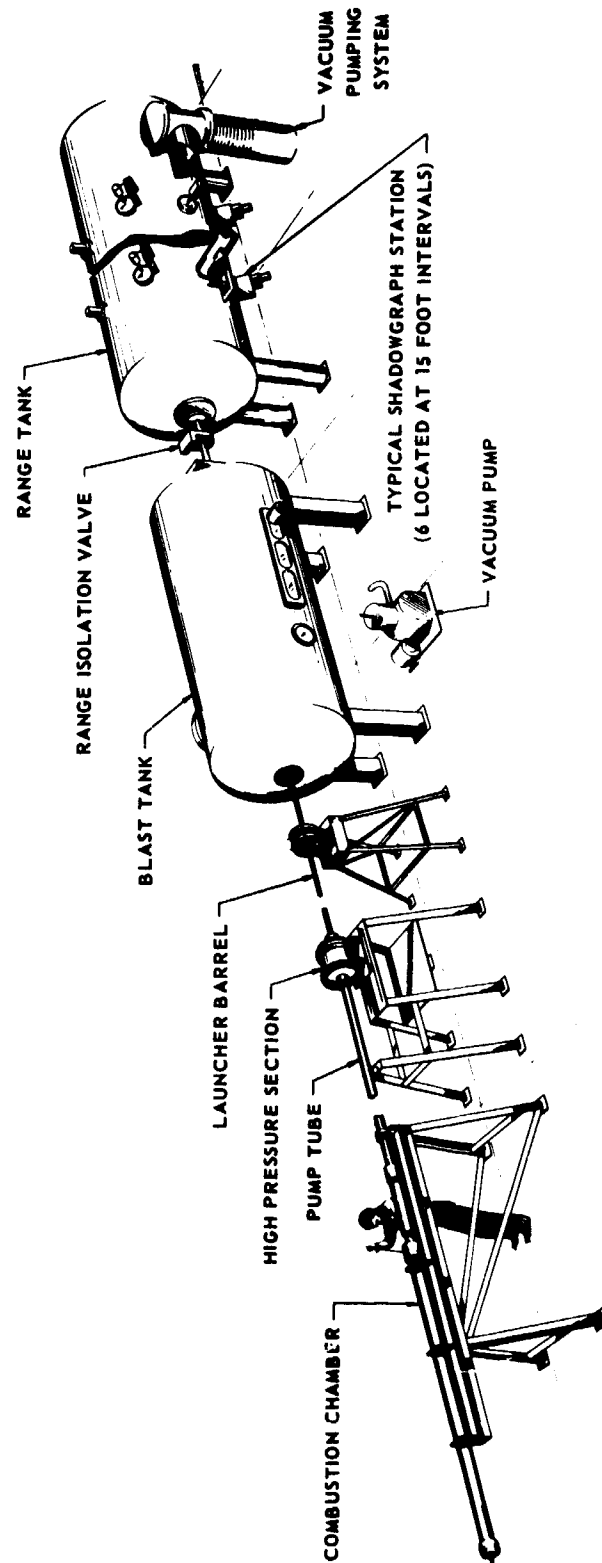
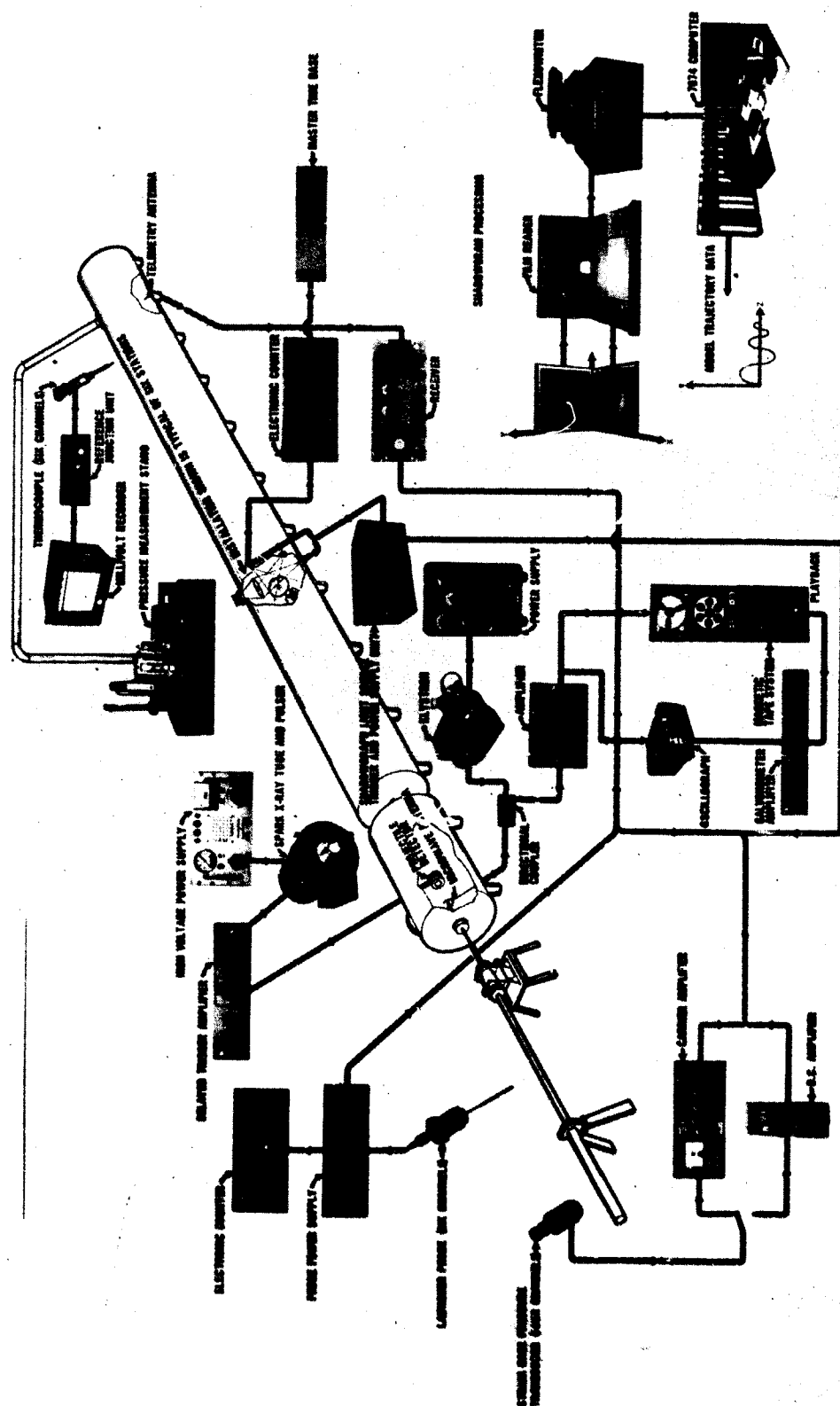


Fig. I-1 VKF 100-ft Hypervelocity Range K



**Fig. I-2 Data Flow - VKF 100-ft Hypervelocity Range K**

**TABLE I-1**  
**VKF 100-FT HYPERVELOCITY RANGE DIMENSIONS AND EQUIPMENT**

<u>Launcher(s)</u>	<u>Inside Diameter (in.)</u>	<u>Length (ft)</u>
Powder Chamber	4.0	2.0
Pump Tube	2.5	15.3
Launch Tube(s)	0.5	16.0
	0.625	16.0
	1.00	16.0
	2.50 (single-stage only)	15.3
<u>Range</u>		
Blast Chamber	72.0	14.0
Range Proper	72.0	100.0
<hr/>		
<u>Permanent Instrumentation Systems</u>	<u>Field of View at Centerline (in.)</u>	<u>No. of Stations</u>
Refocused Shadowgraphs (dual-axis, orthogonal)	12	6
Schlieren	12	1
X-Ray	4 x 32	4
Pressure Measurement	---	1
Temperature Measurements	---	6
		Location: Nominal Distance from Gun Muzzle (ft)
		Station No. 1 @ 23 ft, followed by stations at nominal 15-ft intervals
		28
		3, 6, 14, and 106; others available
		106
		Station No. 1 @ 20 ft, followed by stations at nominal 15-ft intervals

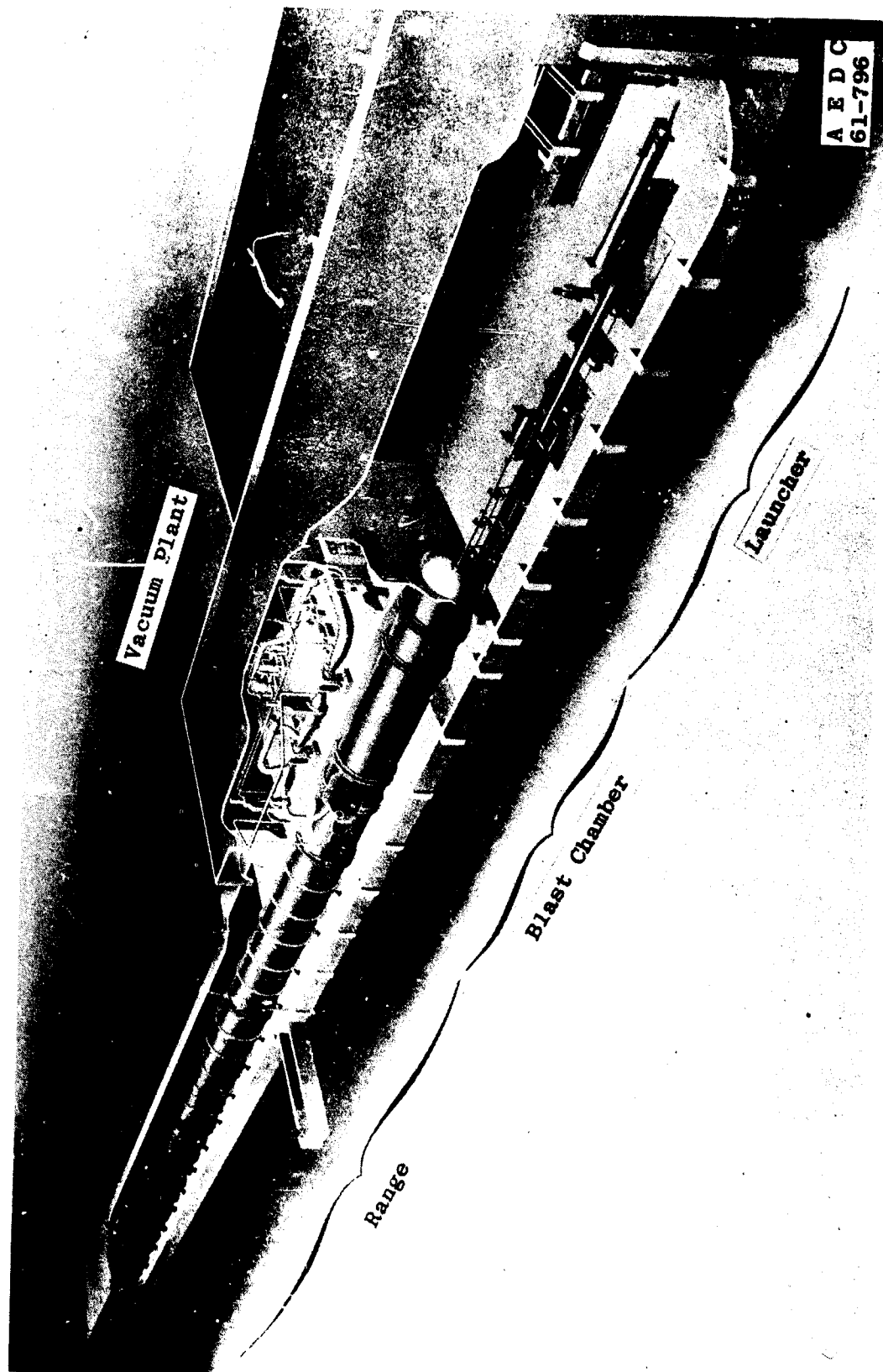


Fig. 1 VKF 1000-ft Hypervelocity Range G

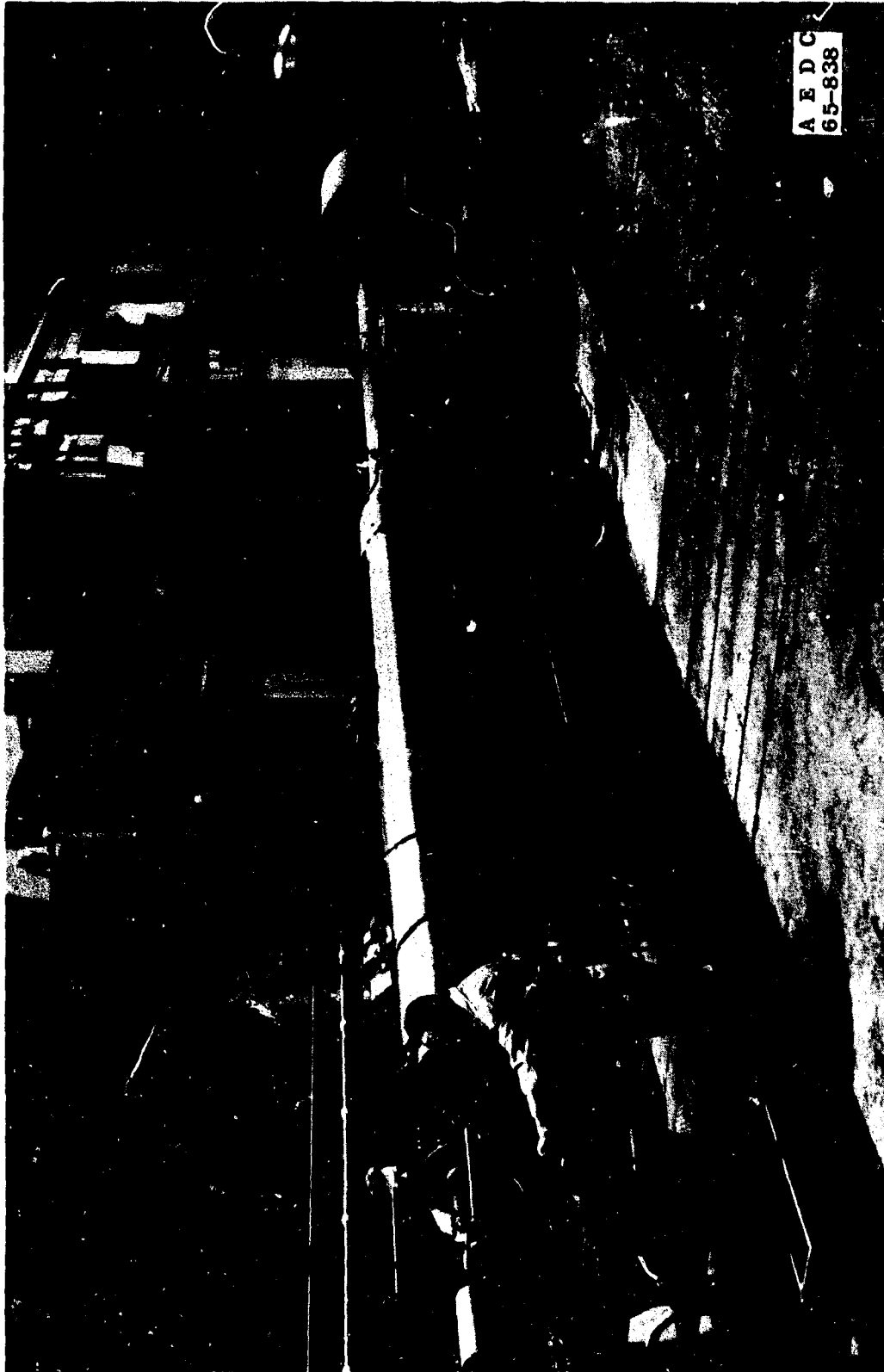
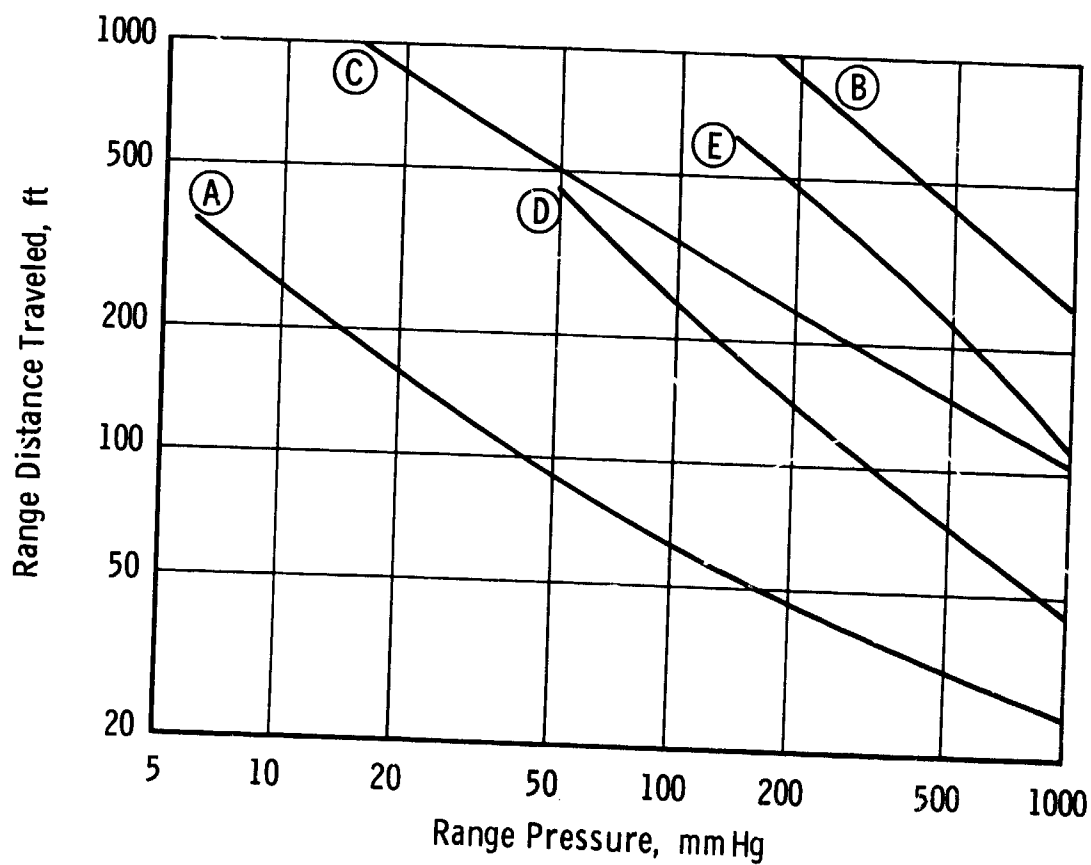


Fig. 2 Launcher - VKF 1000-ft Hypervelocity Range G

Material	Nose Radius, in.	Muzzle Velocity, ft/sec
(A) Re & W Nose	0.030	23,600
(B) Re & W Nose	0.030	12,450
(C) Re & W Nose	0.060	22,500
(D) Cu Nose	0.030	12,450
(E) Ta & W Nose	0.015	11,000



**NOTE:** Results computed for 6- and 6-1/2-deg semi-angle cone models of typical design. Blast chamber pressure of 60-mm Hg used throughout. Distances plotted represent travel beyond the blast tank, in the range proper.

Fig. 3 Distance Traveled before Nose Reached Melting Temperature

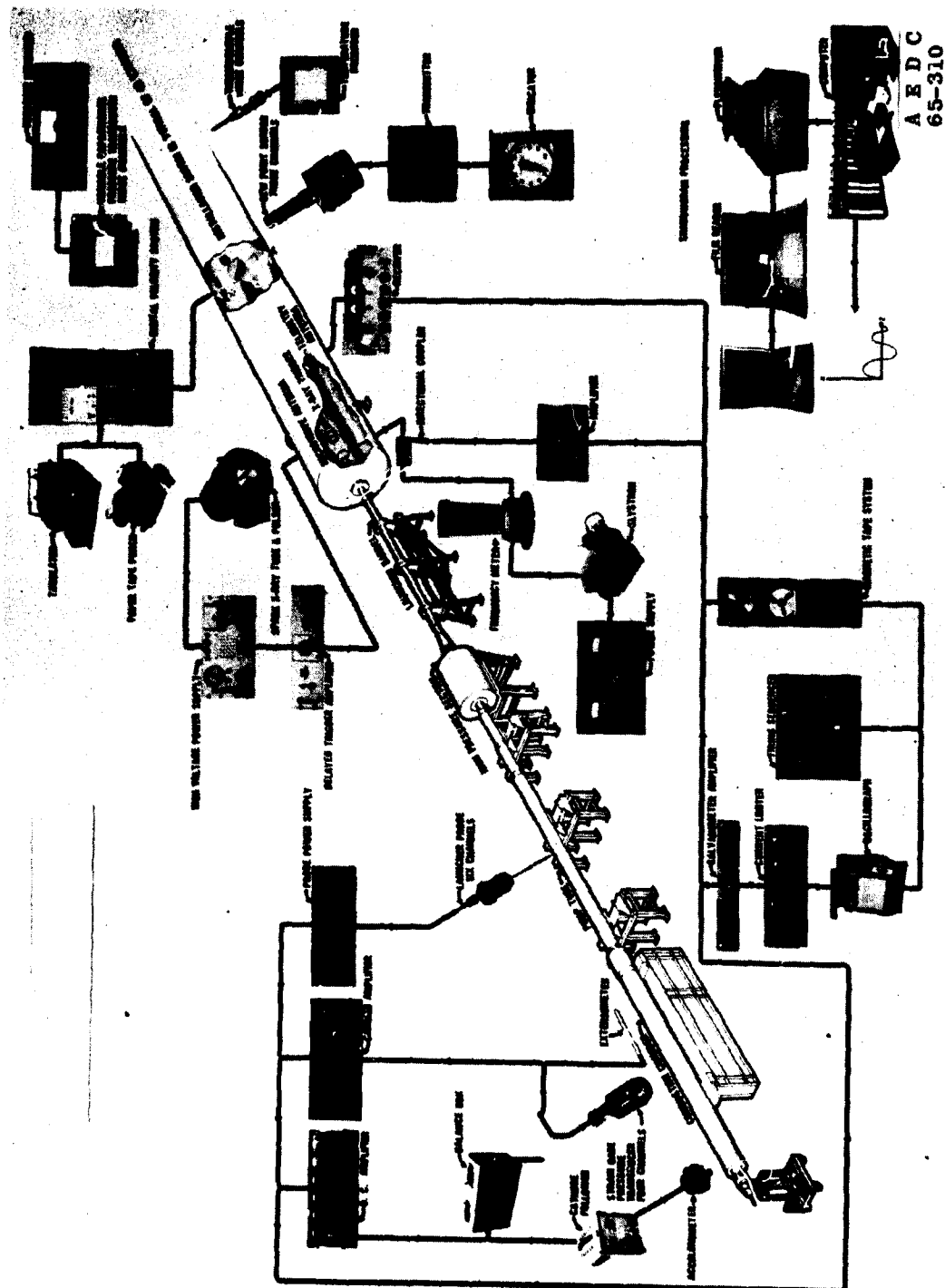
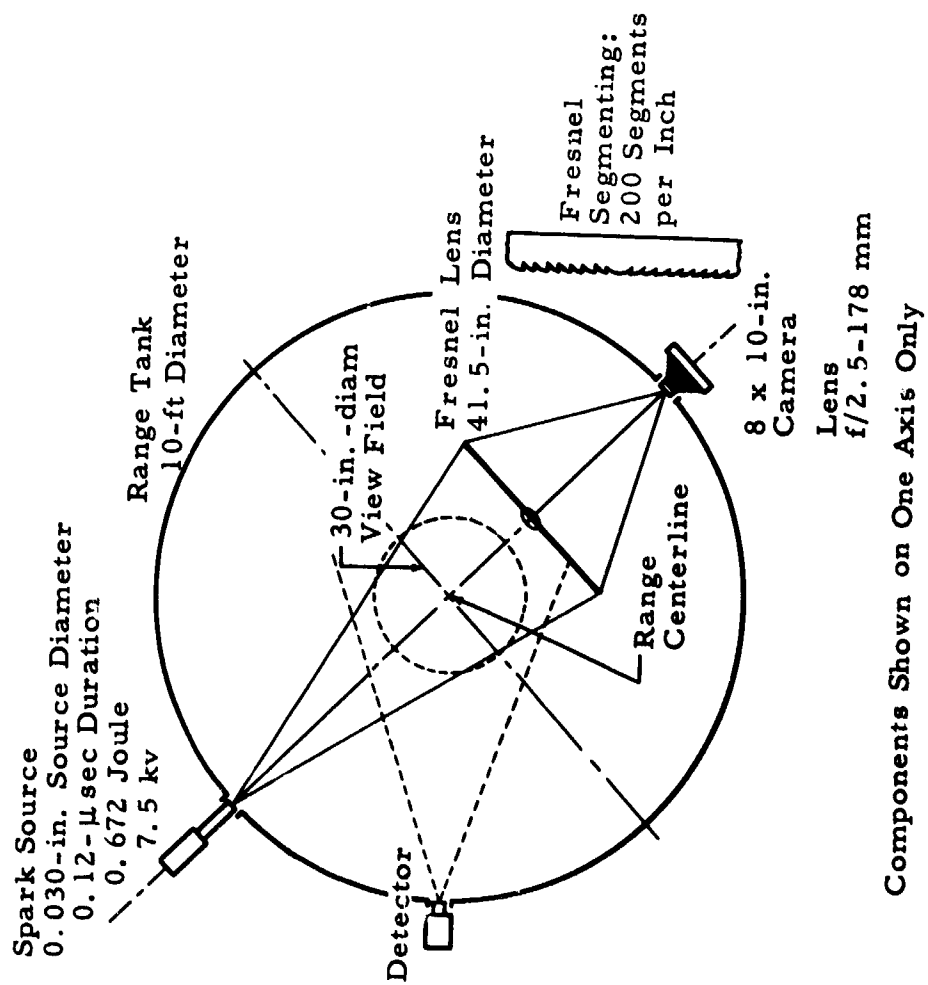


Fig. 4 Routine Data Flow - VKF 1000-ft Hypervelocity Range G



A E D C  
63-1919

Installation Shown Is Typical of 43 Stations

Fig. 5 Shadowgraph Configuration - VKF 1000-ft Hypervelocity Range G

Components Shown on One Axis Only



Fig. 6 Uprange View within VKF 1000-ft Hypervelocity Range G, Showing Shadowgraph Fresnel Lenses

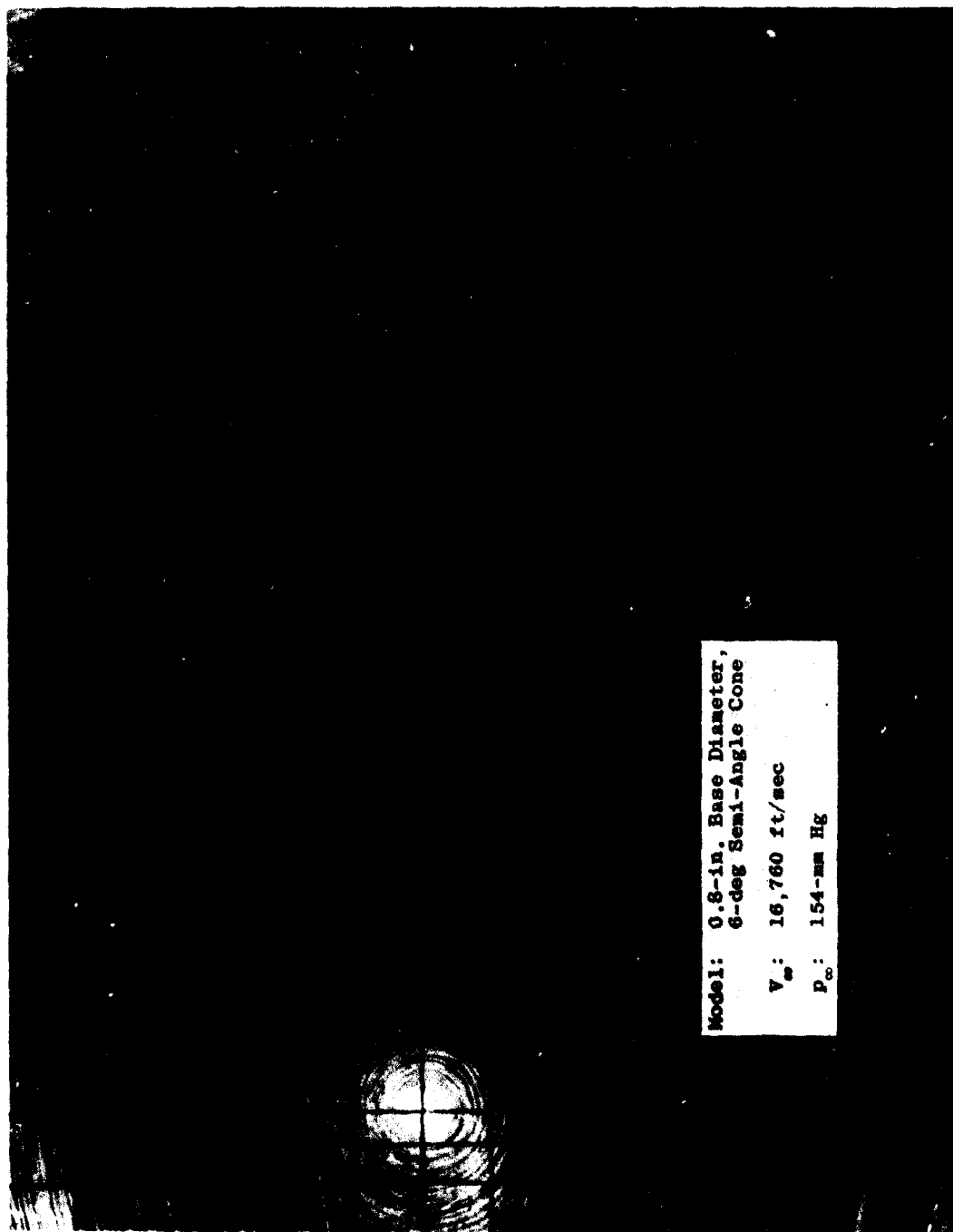


Fig. 7 Shadowgram - VKF 1000-ft Hypervelocity Range G



Fig. 8 X-Ray Shadowgram - VKF 1000-ft Hypervelocity Range G

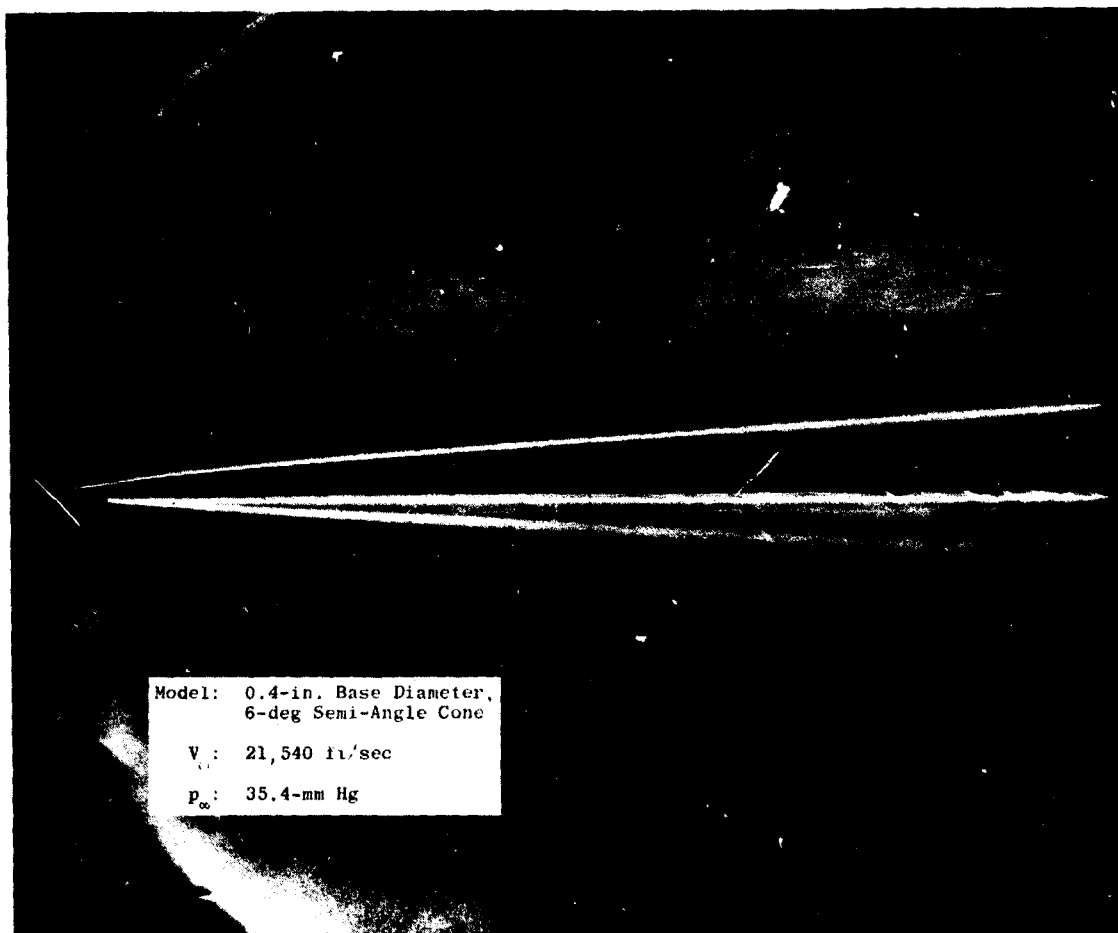
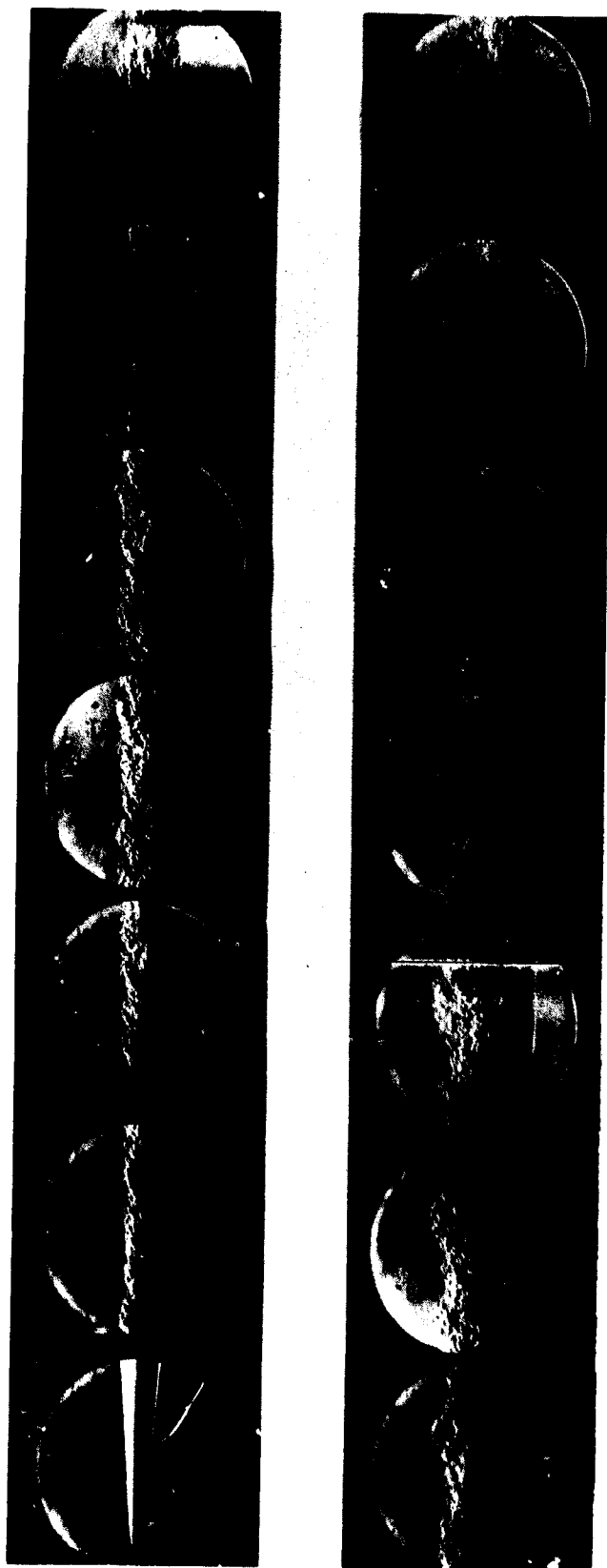


Fig. 9a Single-Frame Schlieren Photograph - VKF 1000-ft Hypervelocity Range G



Model: 0.5-in.-diam Copper Sphere

$V_{\infty}$ : 18,440 ft/sec

$p_{\infty}$ : 65-mm Hg

Spacing between 1st and 2nd Frames: 1,324 Body Diameters

Spacing between Subsequent Frames: 1,260 Body Diameters

Spacing between 1st and Final Frames: 16,444 Body Diameters

Fig. 9b Turbulent Wake behind a Hypervelocity Sphere

Model: 0.125-in.-diam  
Copper Sphere  
 $V_{\infty}$ : 26,200 ft/sec  
 $p_{\infty}$ : 19.6-mm Hg  
Spacing between 1st and  
2nd Frames: 450 Body Diameters  
Spacing between Subsequent  
Frames: 250 Body Diameters  
Spacing between 1st and Final  
Frames: 3950 Body Diameters

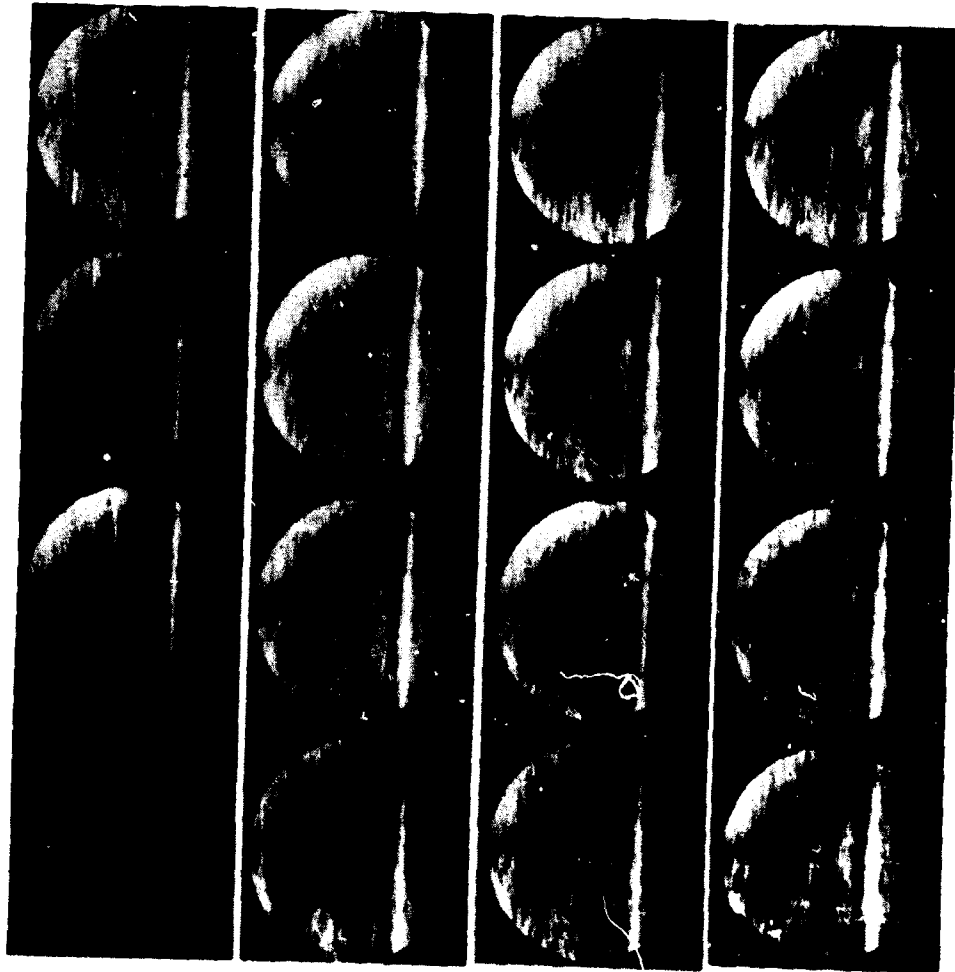
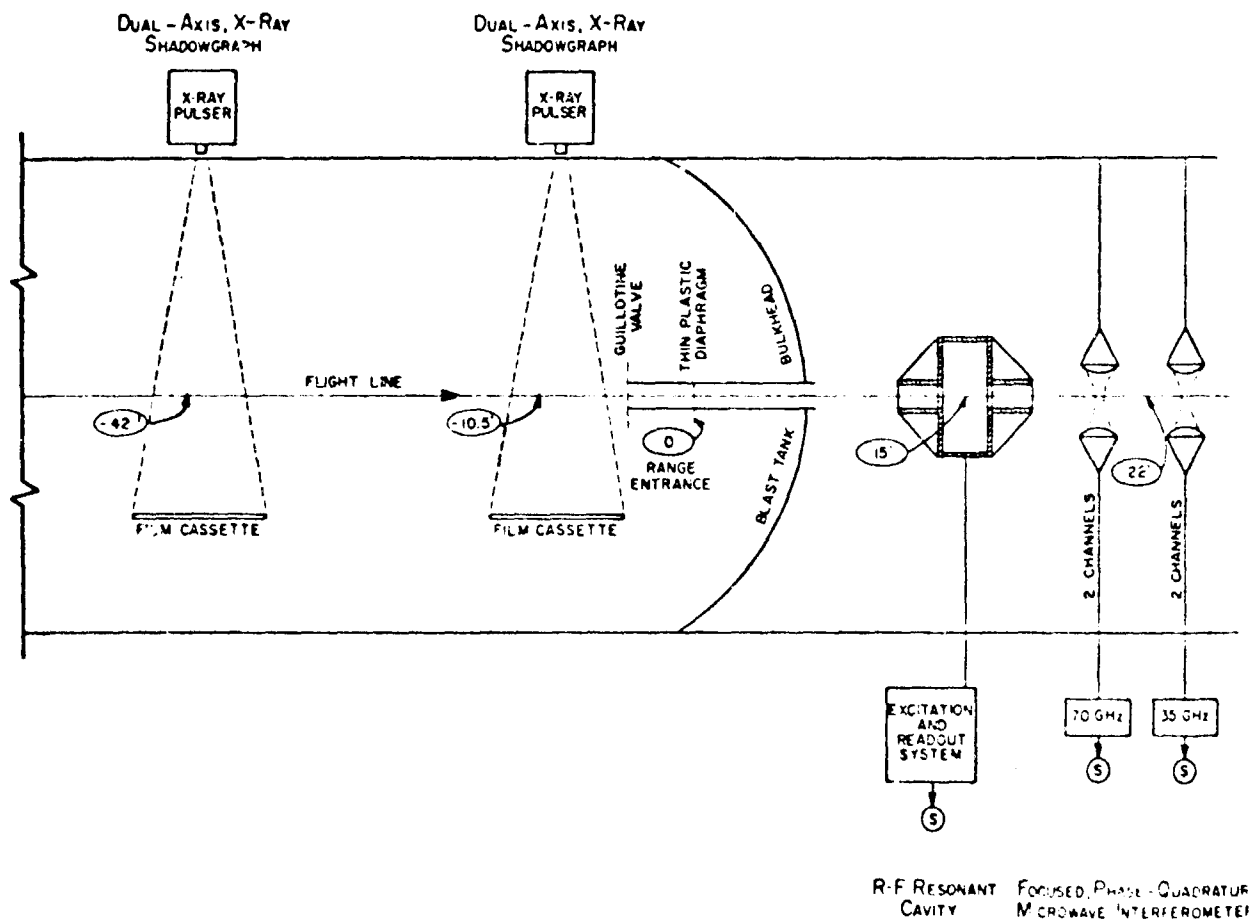
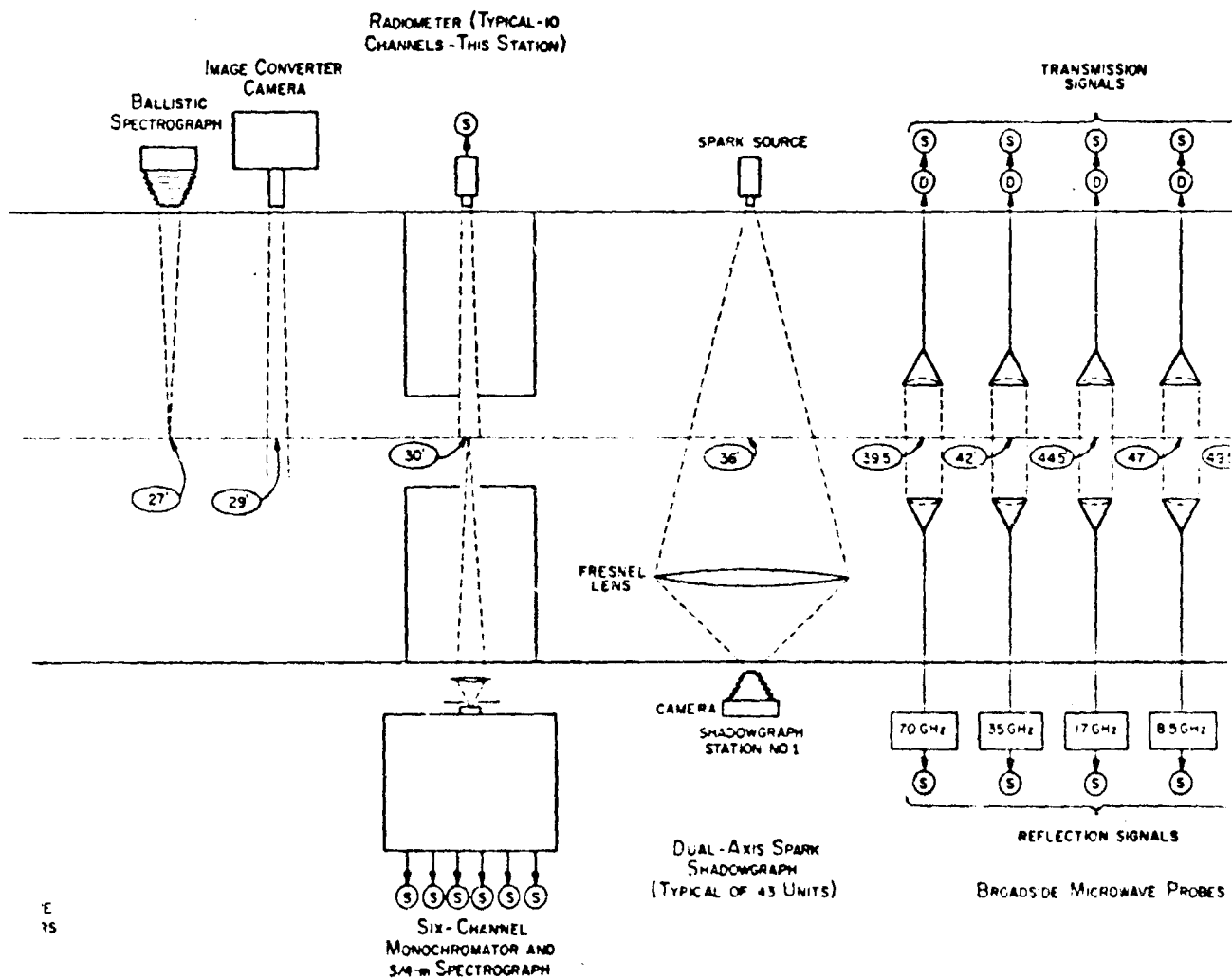


Fig. 9c Inviscid Wake behind a Hypervelocity Sphere

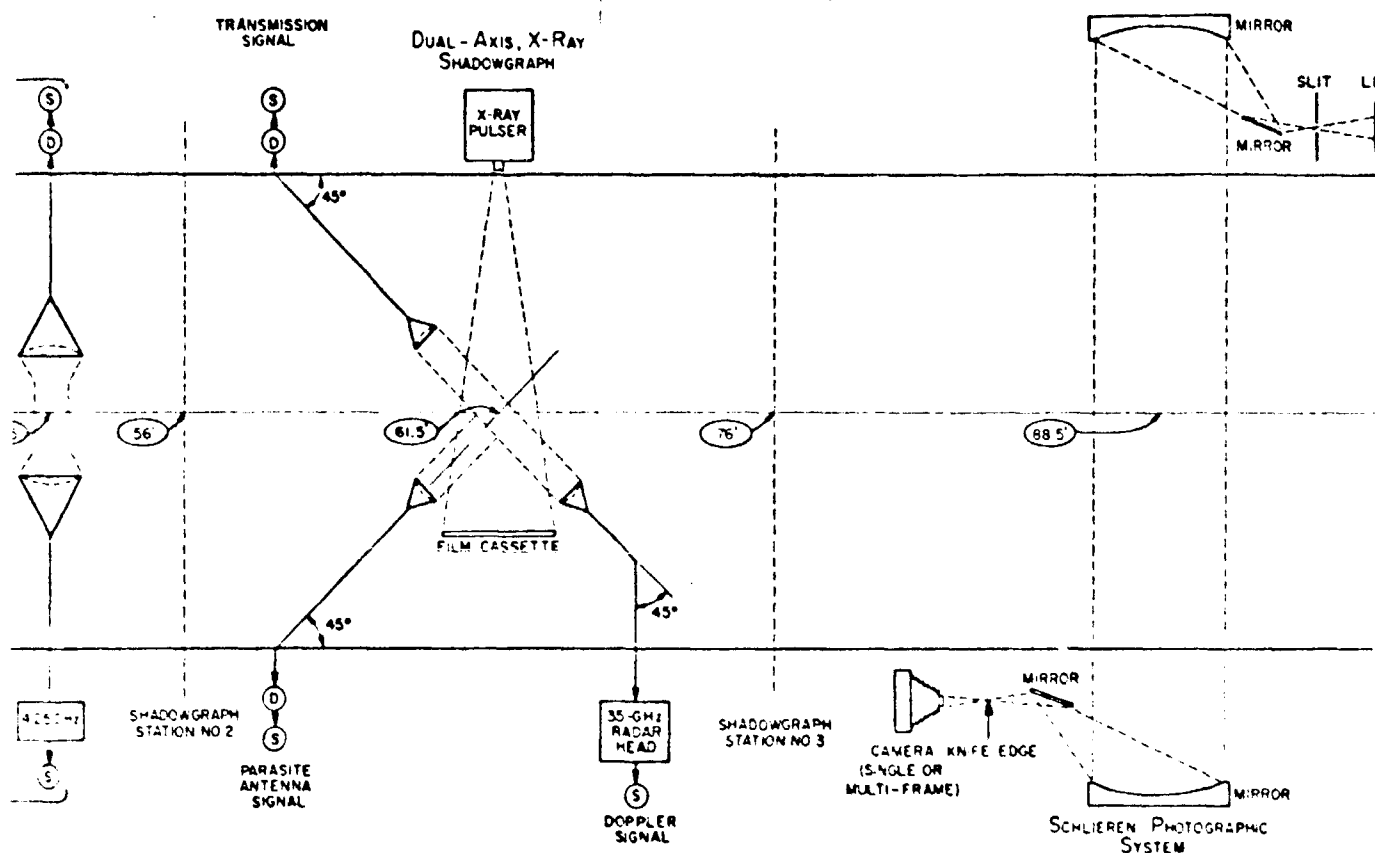
A



B

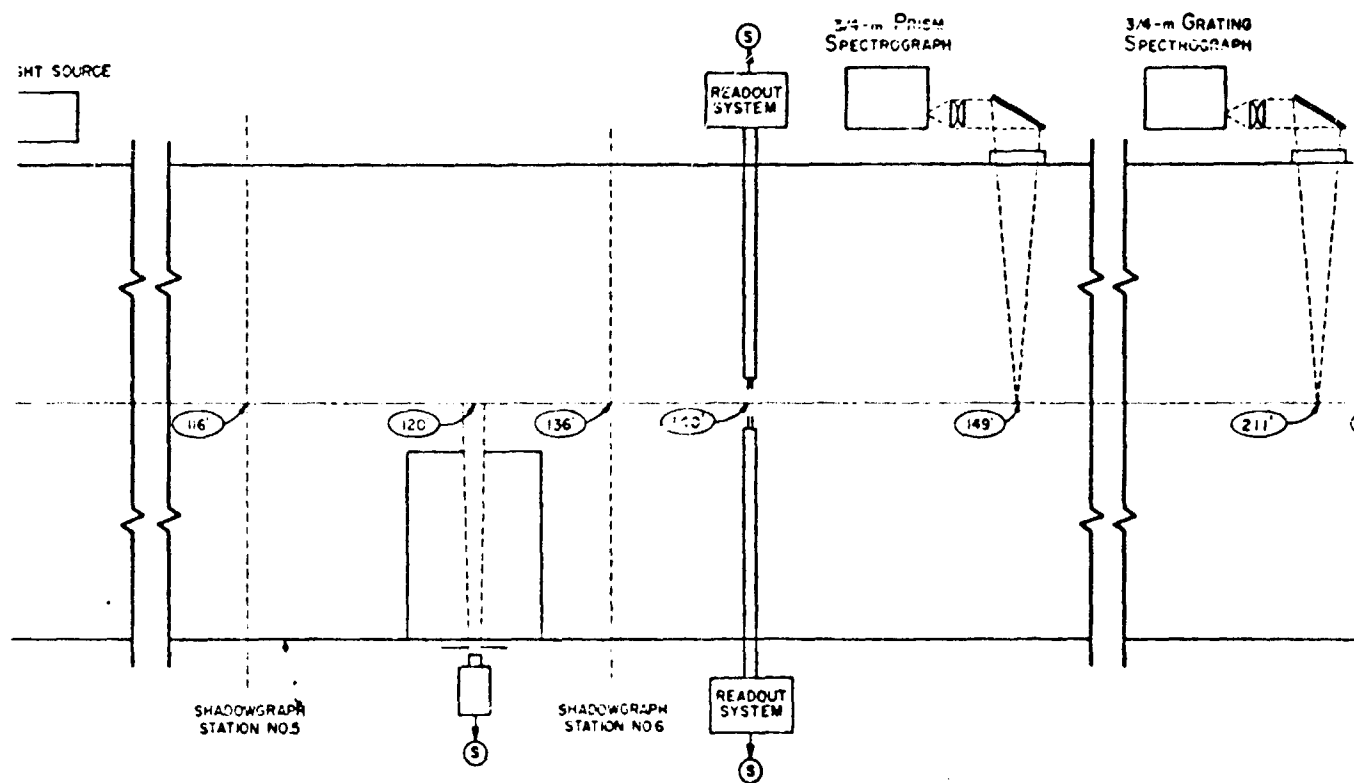


C



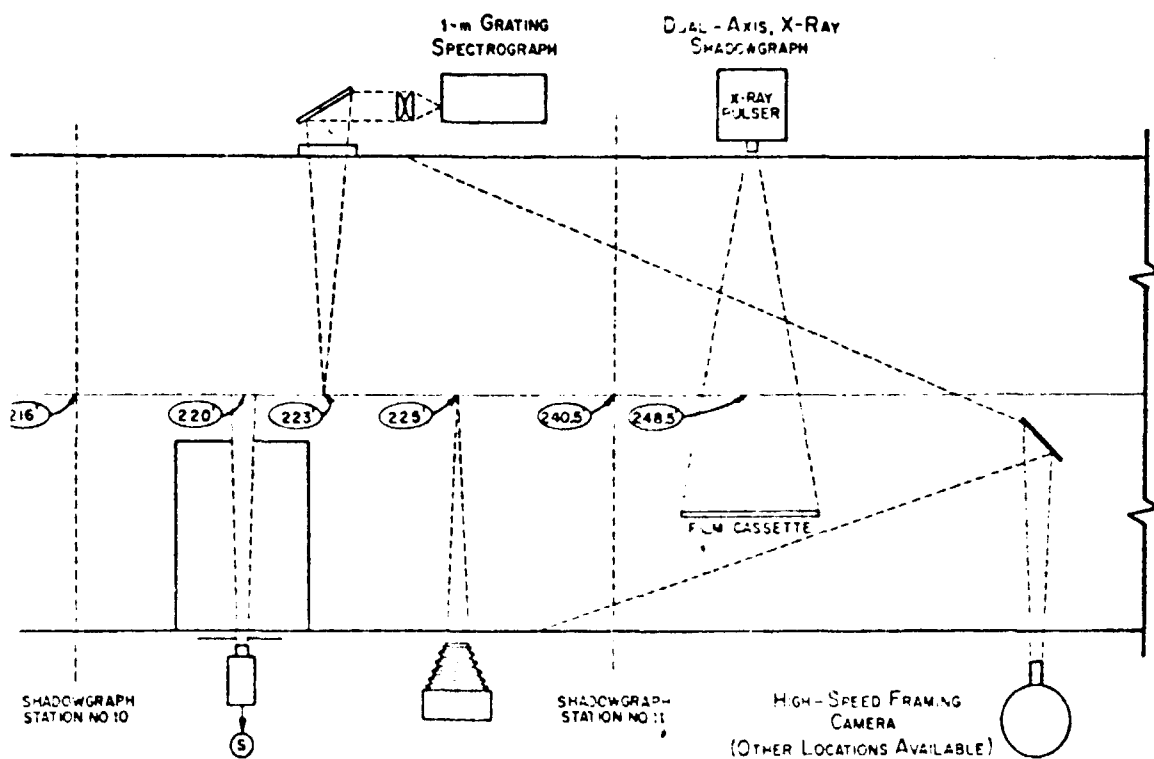
OBLIQUE DOPPLER RADAR

D



RADIOMETER (TYPICAL-2  
CHANNELS - THIS STATION)

LANGMUIR PROBES



NOTES

1. NOT TO SCALE
2. (X) CR-STA. DETECTOR
3. (S) OSCILLOSCOPE
4. (XX) DENOTES DISTANCE TO NEAREST 100 FEET FROM RANGE ENTRANCE

INSTRUMENTATION  
EQUIPMENT  
VKF 1000-ft HYPERVELOCITY  
RANGE G  
Fig 10a

F

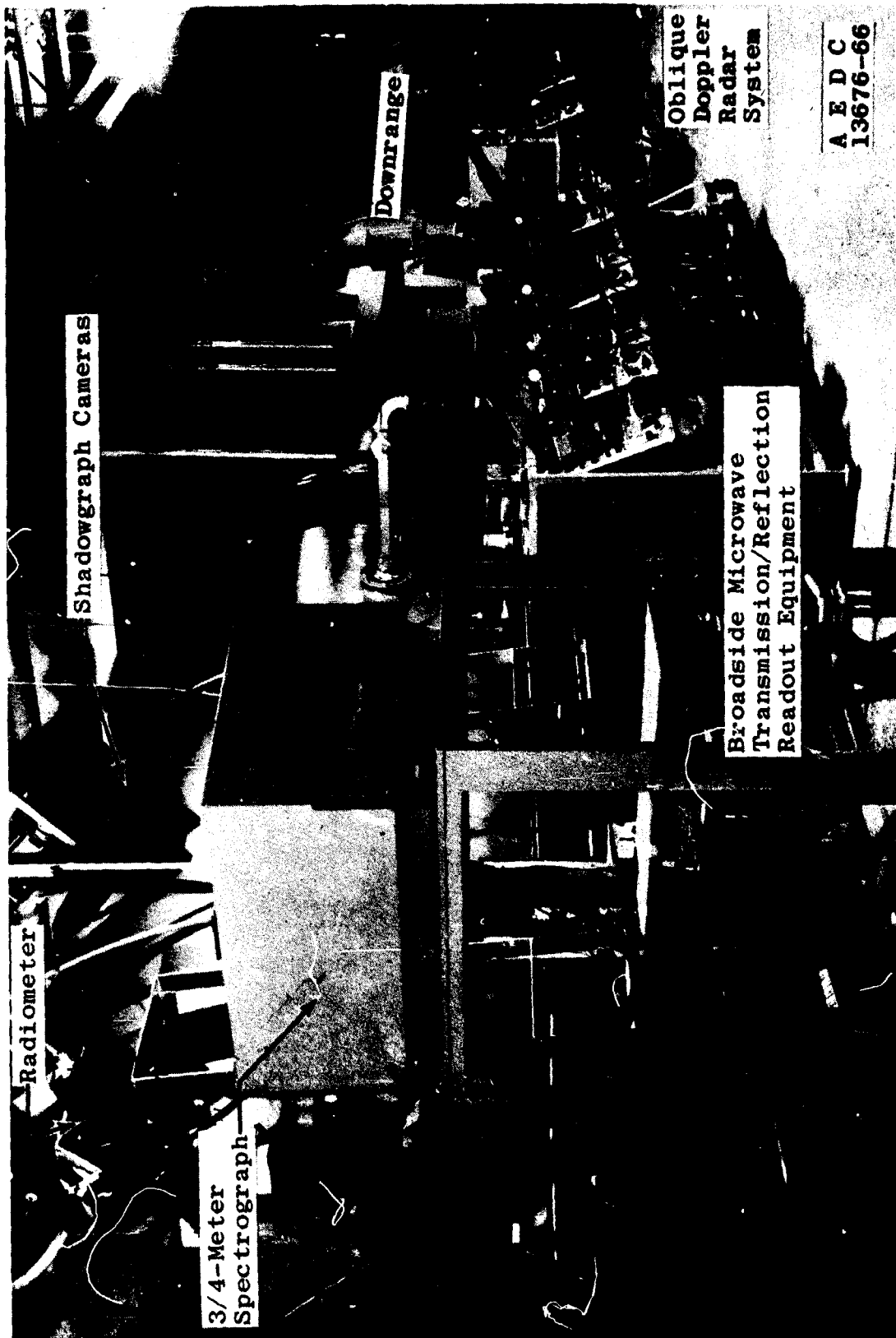


Fig. 10b Exterior View - VKF 1000-ft Hypervelocity Range Instrumentation Equipment

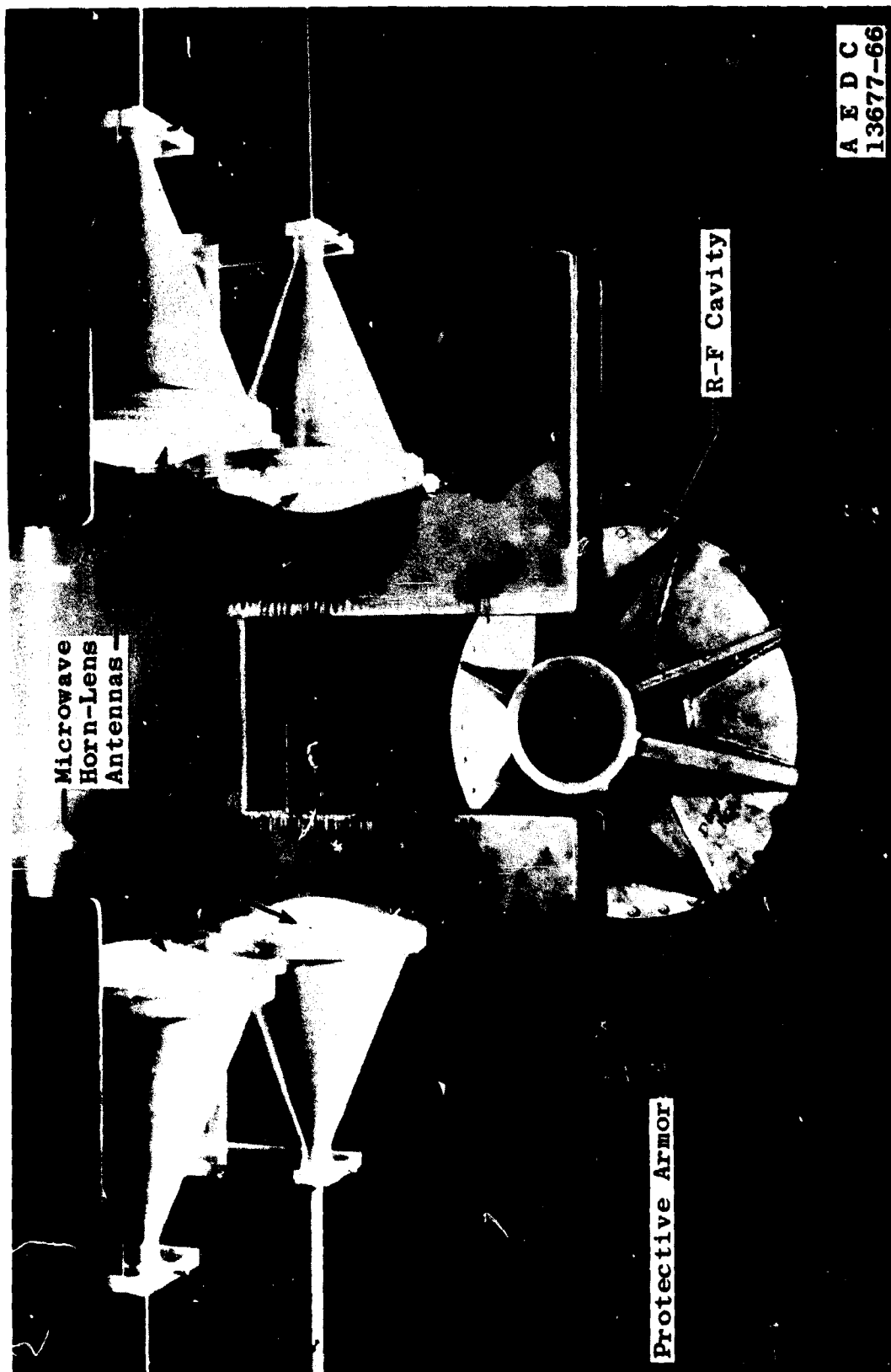
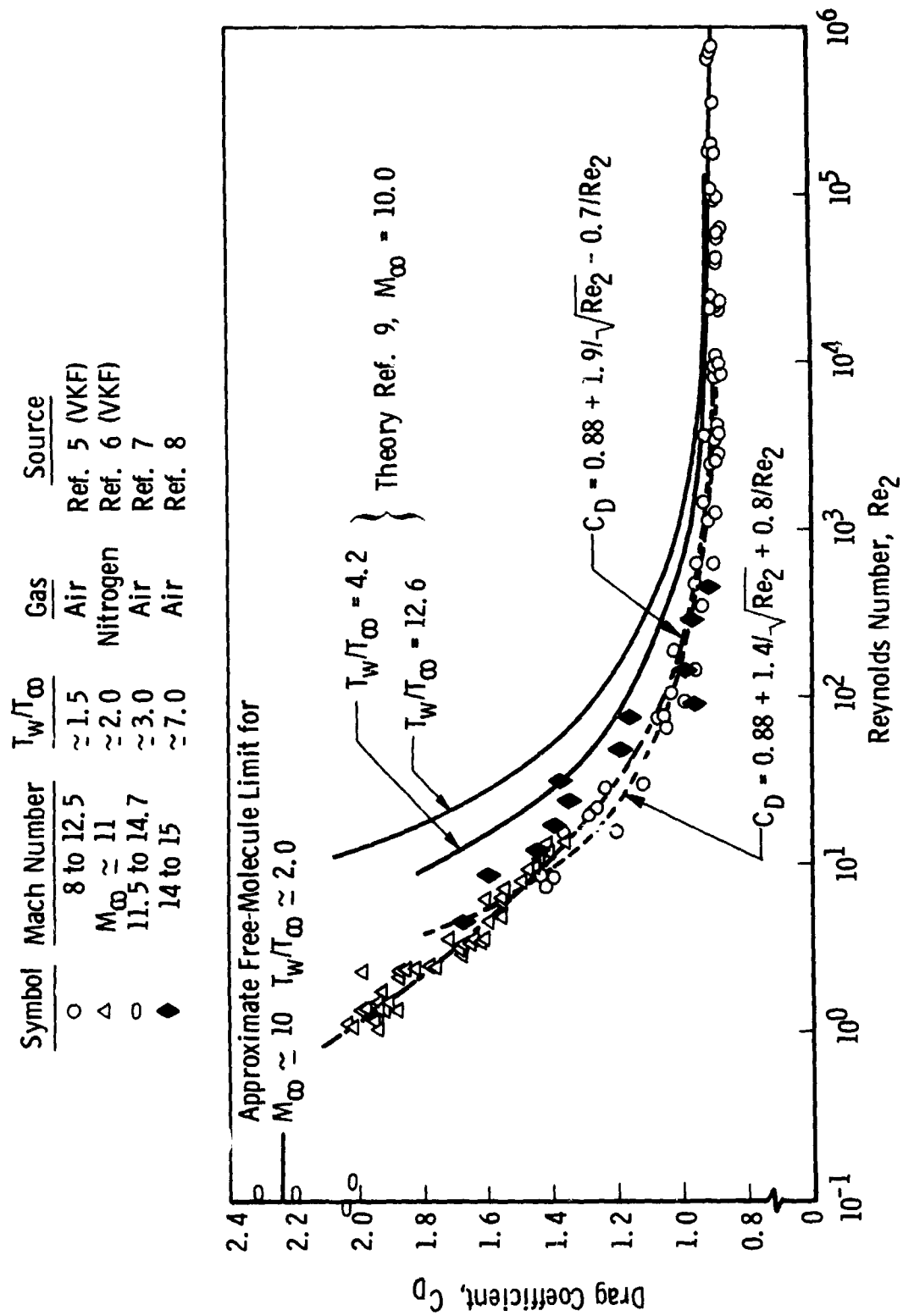
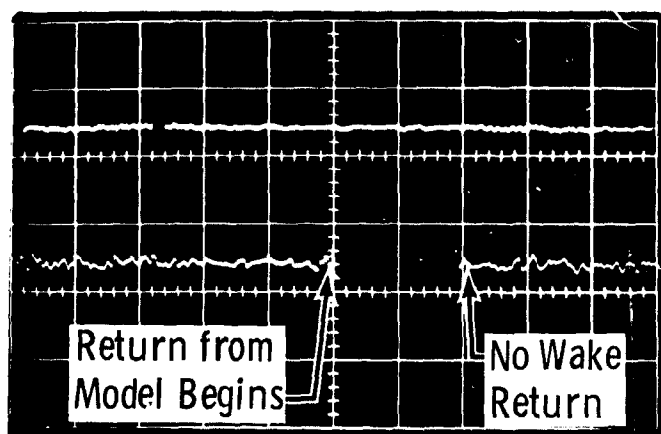


Fig. 10c Resonant R-F Cavity and Focused Microwave Probes - Uprange View

Fig. 11 Variation of Support-Free Sphere Drag Coefficient with Reynolds Number ( $8 < M_\infty < 15$ )



DIRECT SWEEP

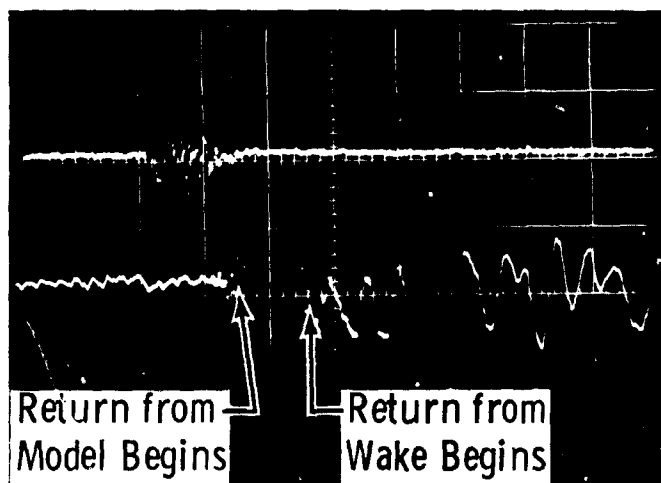
Vertical: 200 mv/cm  
Horizontal: 100  $\mu$ sec/cm

DELAYED SWEEP

Vertical: 100 mv/cm  
Horizontal: 10  $\mu$ sec/cm

0.125-in.-diam Tungsten Carbide Sphere  
 $V_{\infty}$ : 19,400 ft/sec  
 $p_{\infty}$ : 200-mm Hg

a. Nonablating Model



DIRECT SWEEP

Vertical: 200 mv/cm  
Horizontal: 100  $\mu$ sec/cm

DELAYED SWEEP

Vertical: 100 mv/cm  
Horizontal: 10  $\mu$ sec/cm

0.125-in.-diam Steel Sphere  
 $V_{\infty}$ : 17,700 ft/sec  
 $p_{\infty}$ : 200-mm Hg

b. Ablating Model

Fig. 12 35-GHz Oblique Doppler Radar Signals

Oblique Focused Doppler Radar

Symbol	$V_{\infty}$ kft/sec	$P_{\infty}$ mm Hg	Material	Diameter, in.	Source
☆	15.6-21.0	35	Aluminum	0.25-0.437	Ref. 11 (VKF)
★	17.4-18.5	200	Steel	0.125	
●	20.5	50	Nylon	0.125	
◆	17.0	734	Tungsten Carbide	0.125	
---	17.6-19.6	50-100	Copper	0.2~0.6	Ref. 10

Schlieren

△	10.0-11.0	100	Aluminum	0.437	Ref. 11 (VKF)
---	7.6	≈ 760	Aluminum	0.50	Ref. 12
—	Theory				Ref. 14

Luminosity - Drum Camera Technique

---	13.5-14.0	40~60	Lexan		Ref. 13
-----	-----------	-------	-------	--	---------

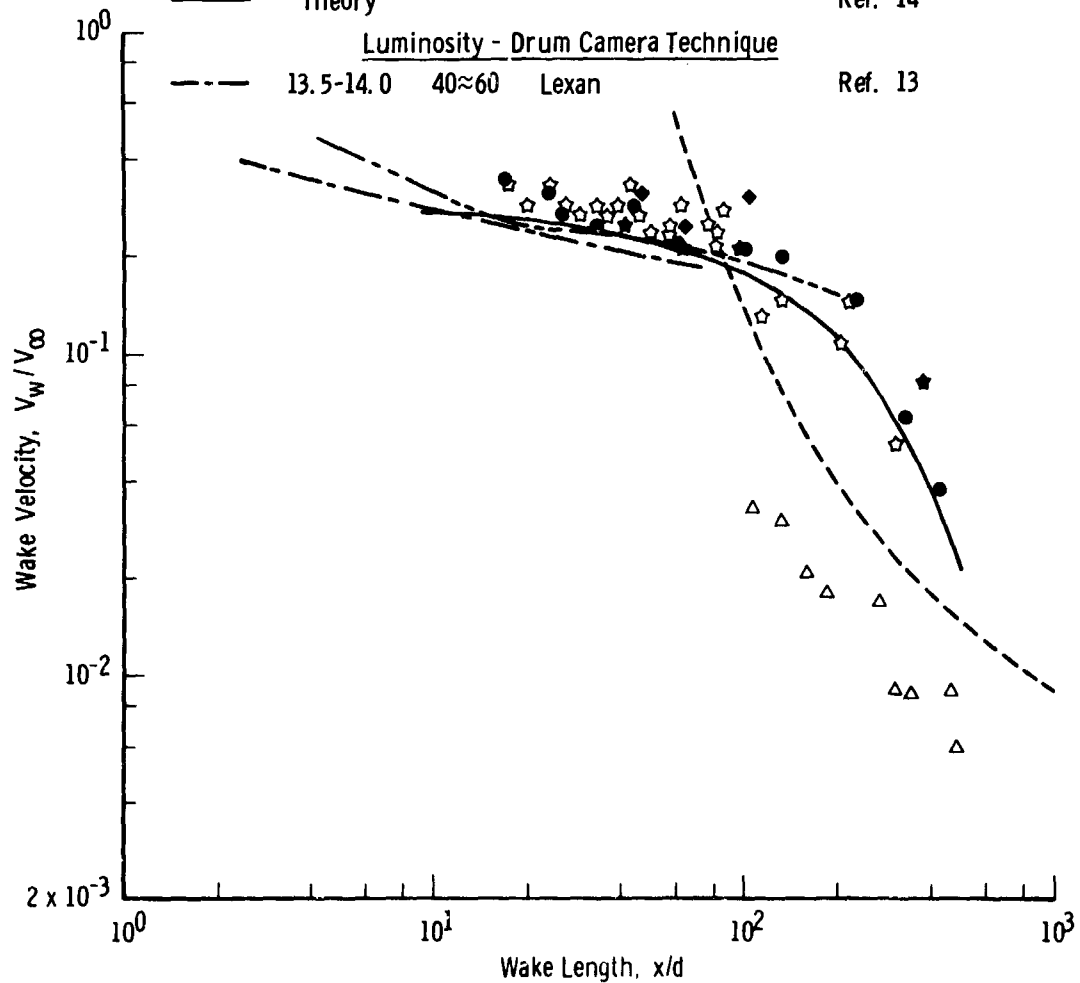


Fig. 13 Wake Velocity behind a Sphere

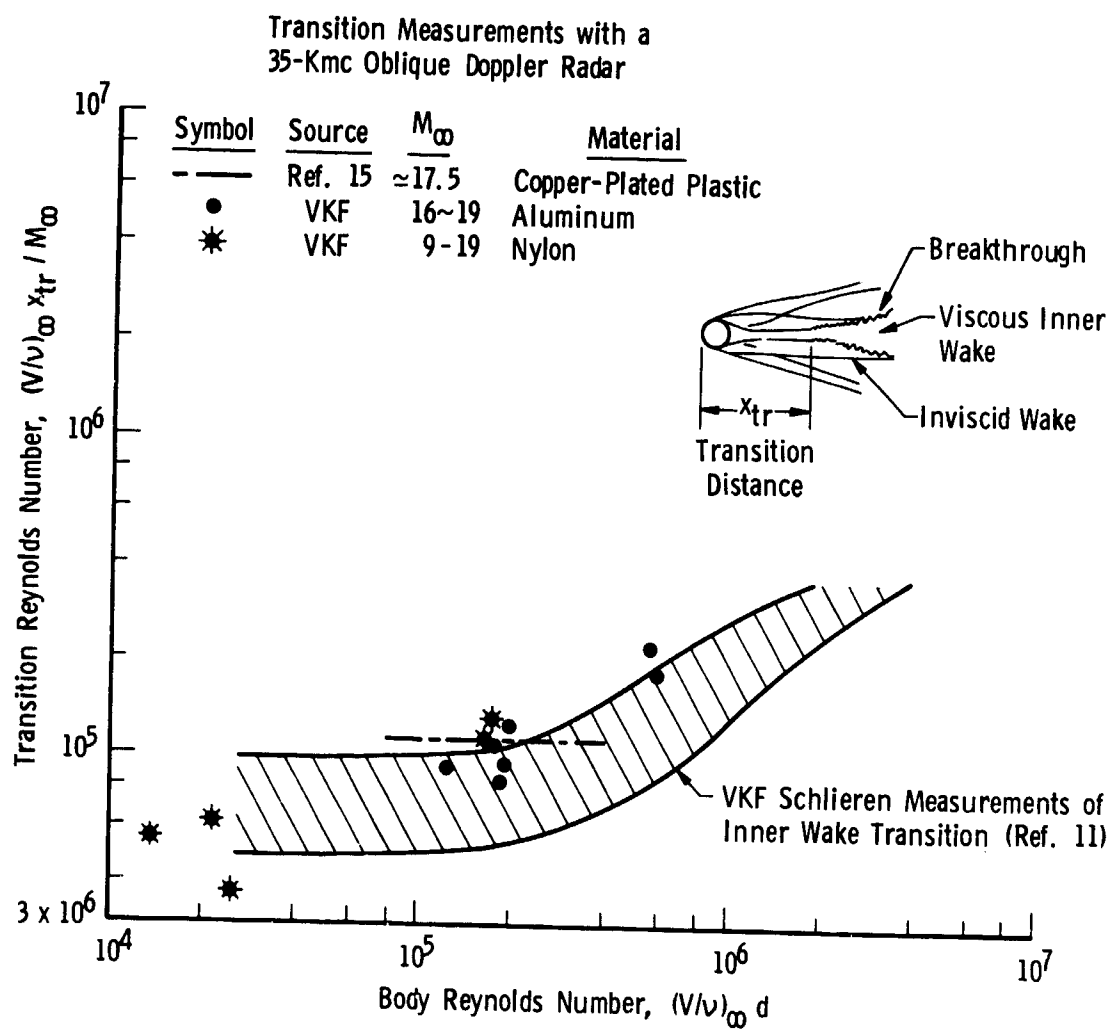


Fig. 14 Comparison of Schlieren and Microwave Measurements of Inner Wake Transition Distance

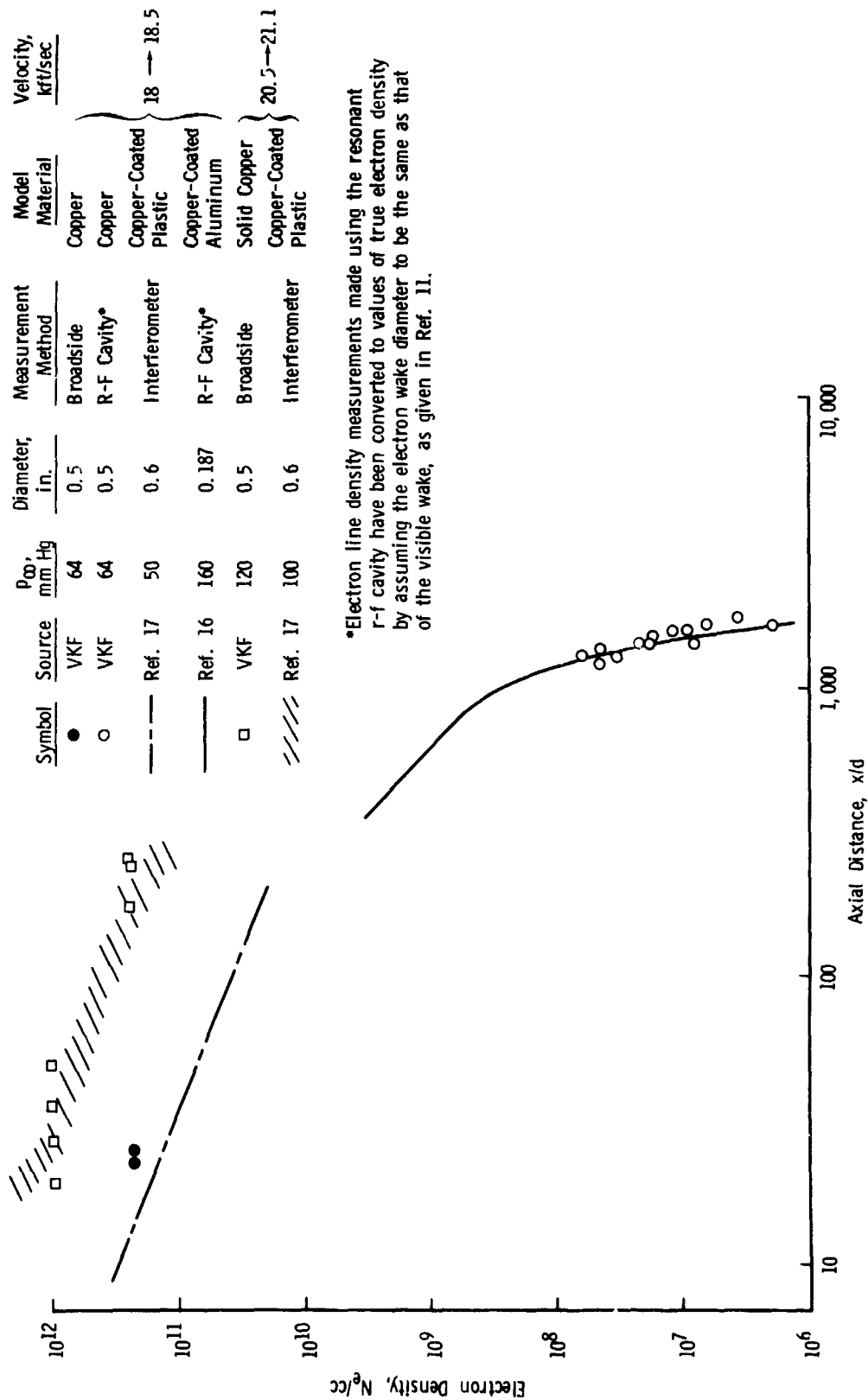


Fig. 15 Electron Density Decay in Wakes of Nonablating Spheres

**NOTE:** Solid curves are calculated forcings, based on  $V_{\infty} = 16,000$  ft/sec and  $p_{\infty} = 76$  mm Hg, for all slit widths. Max. value of radiance forcing shown for 6.4-mm slit was adjusted to equal peak value of radiometer data; other forcing functions adjusted in equal ratio.

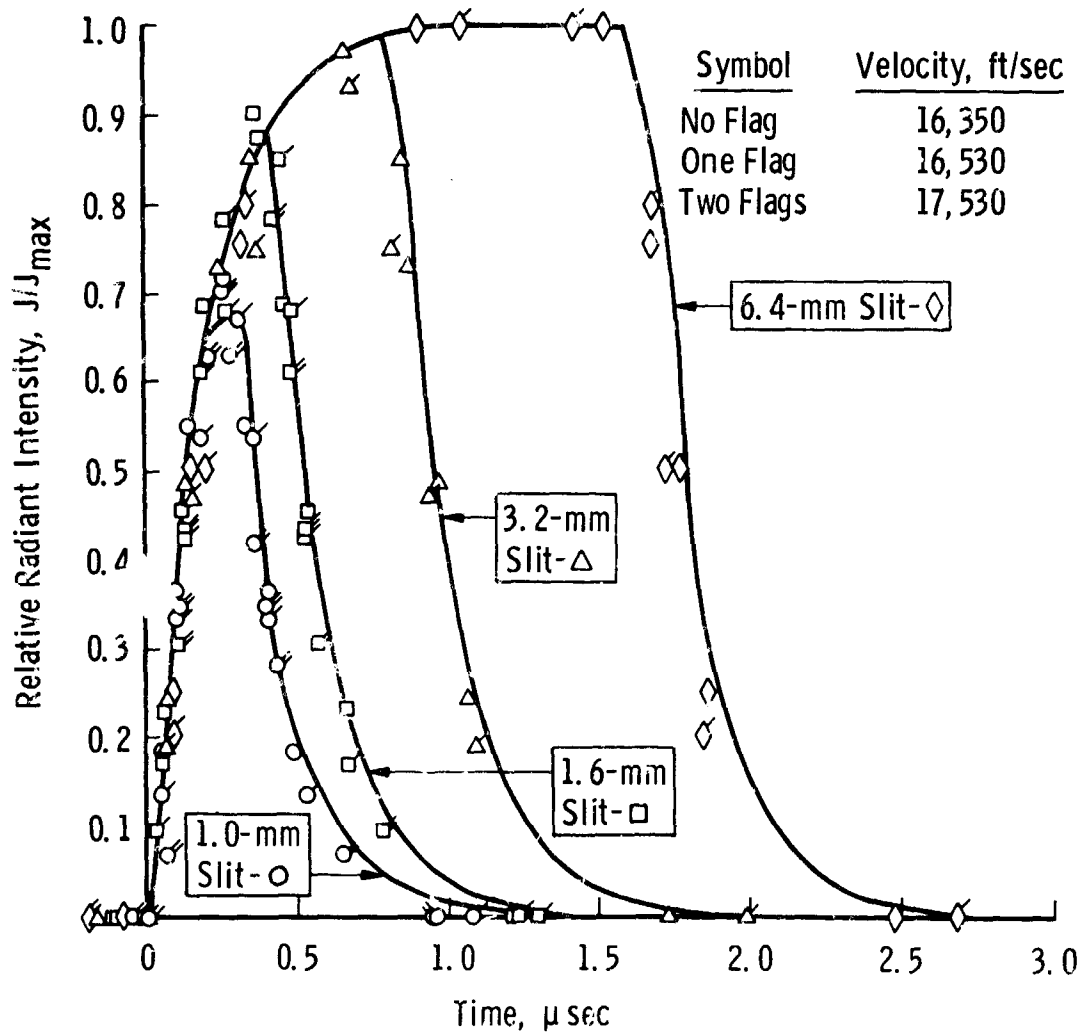


Fig. 16 Comparison of Calculated Forcing and Measured Response of Narrow-Slit Radiometer

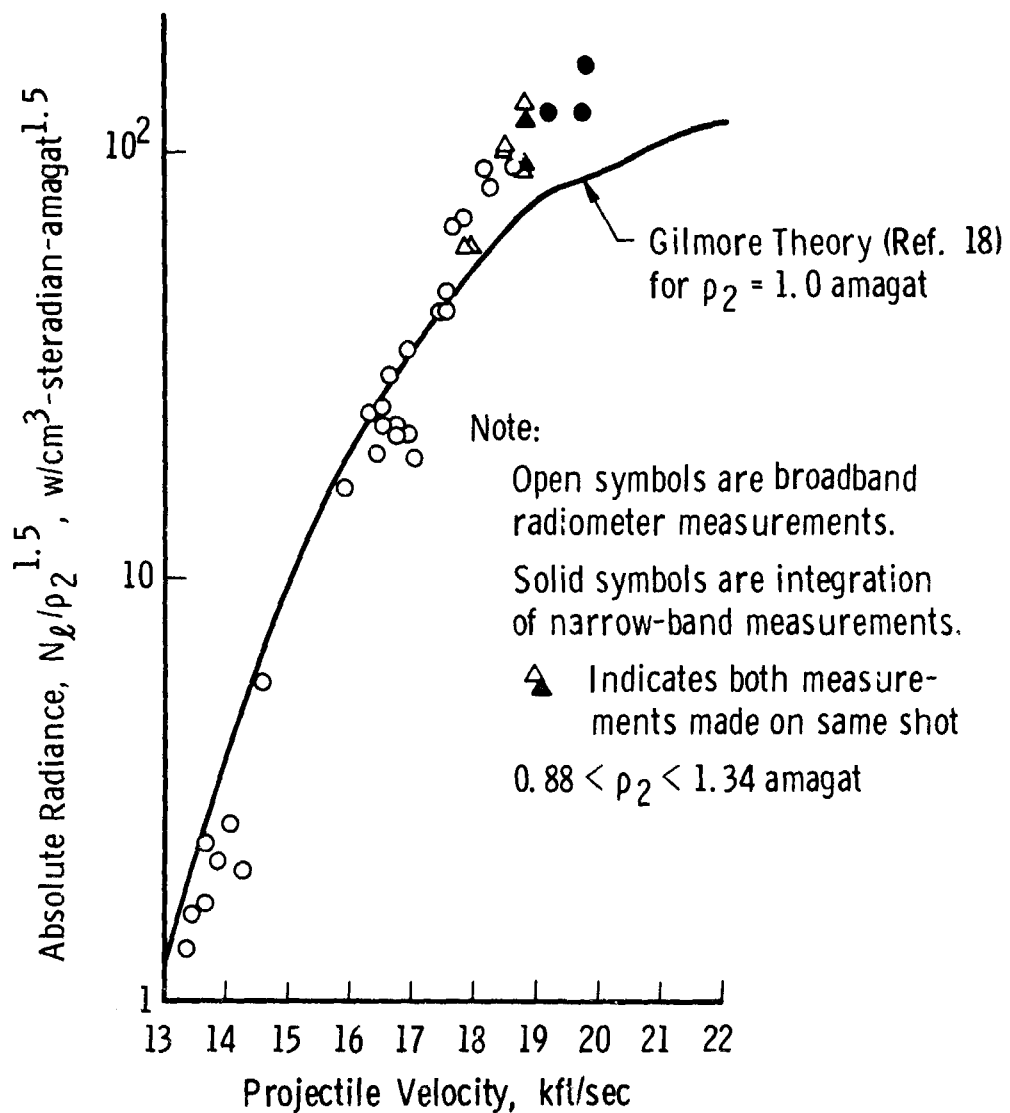


Fig. 17 Measurements of Total Radiance of Equilibrium Shock Cap of Sphere

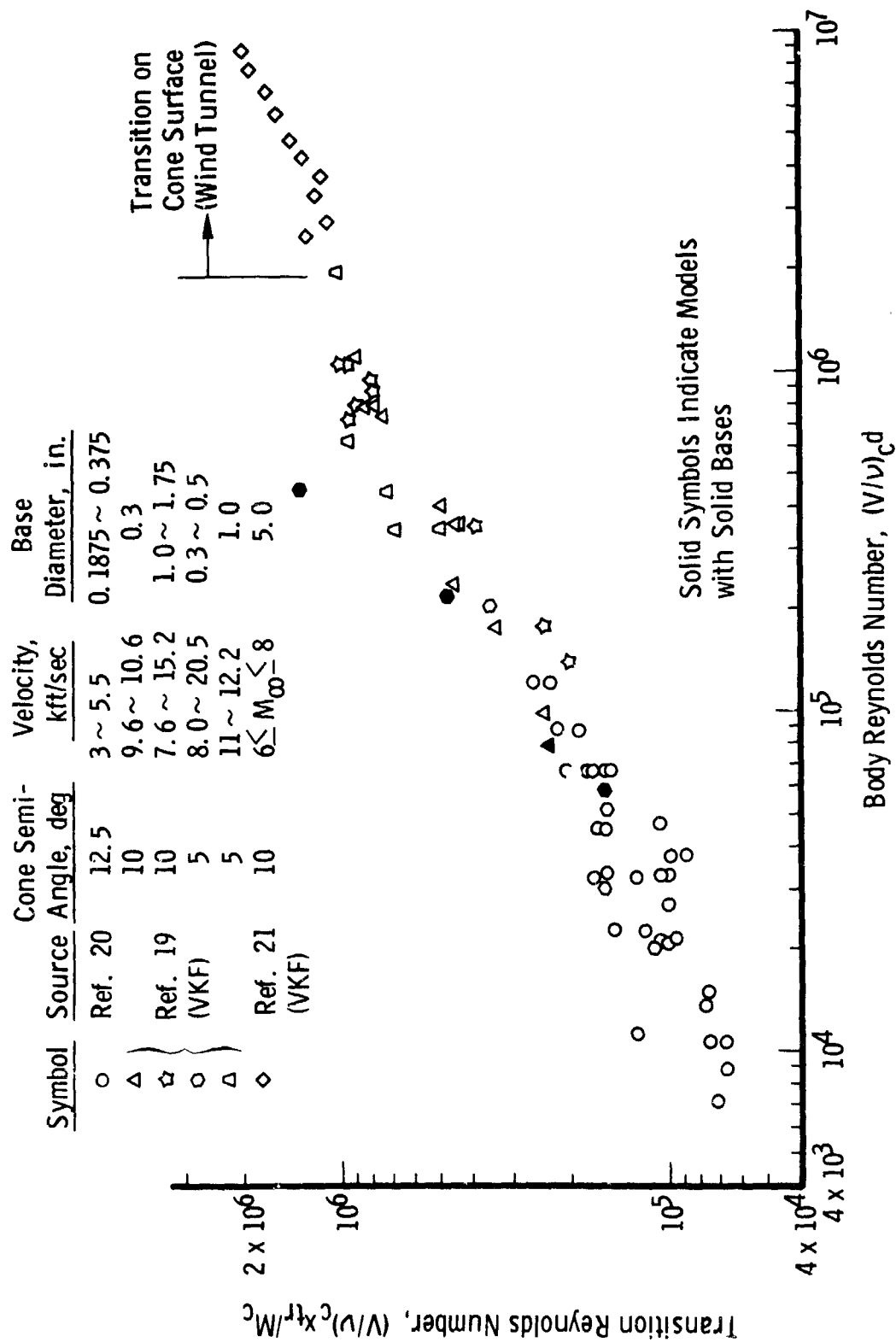


Fig. 18 Transition Reynolds Number Variation with Body Reynolds Number

TABLE I  
VKF 1000-FT HYPERVELOCITY RANGE DIMENSIONS AND EQUIPMENT

<u>Launcher</u>	<u>Inside Diameter (in.)</u>	<u>Length (ft)</u>	
Powder Chamber	14.2	4.0	
Pump Tube	3.0	50.5	
Launch Tube	2.5	41.7 (nominal minimum)	
<u>Range</u>			
Blast Chamber	118.0	85.5	
Range Proper	120.0	917.5	
-----			
<u>Standard Instrumentation Systems</u>	<u>Field of View at Range Centerline (in.)</u>	<u>No. of Stations</u>	<u>Location: Nominal Distance from Gun Muzzle (ft)</u>
Refocused Shadowgraphs (dual-axis, orthogonal)	30	43	Station No. 1 @ 104 ft, followed by stations at nominal 20-ft intervals
Schlieren	30	1	156
X-Ray	12 x 21	5	26, 58, 132, and 318; others available
Pressure Measurements	---	3	522,
Temperature Measurements	---	3	522,
Dew-Point Measurements	---	3	522,

TABLE II  
LAUNCHING CAPABILITY, TYPICAL MODELS

<u>Configuration</u>	<u>Size</u>	<u>Model Material</u>	<u>Model Weight (gm)</u>	<u>In-Gun Weight* (gm)</u>	<u>Peak Velocity** (ft/sec)</u>
Right-Circular Cylinder	2.5-in. diam by 1.3-in. long	Plastic	---	130	23,000
Sphere	0.5-in. diam	Copper	9.5	140	23,000
15° Semi-angle Cone	1.0-in. base diam	Aluminum	16.0	150	22,000
6° Semi-angle Cone	0.4-in. base diam	Composite Metals	5.2	158	22,100
10° Semi-angle Cone	0.5-in. base diam	Composite Metals	4.1	149	21,800
10° Semi-angle Cone	1.75-in. base diam	Aluminum	81.6	386	14,000
5° Semi-angle Cone	1.5-in. base diam	Aluminum	128.5	498	12,000

\*Weights shown here are those of the model plus the sabot which adapts it to the bore of the launcher.

\*\*Performance limits shown here existed in September 1966. Launcher performance is the subject of a continuing development program; peak velocities at which given projectile configurations can be reliably launched increase as the development work progresses.

TABLE III  
MICROWAVE AND R-F CAVITY MEASUREMENT SYSTEM CHARACTERISTICS

System	Operating Frequency (GHz)	Typical Beam Width at Range Centerline* (10-db points) (in.)	Electron Cutoff Density at Operating Frequency (e/cm <sup>3</sup> )	Measurable Range of Electron Density for 1.0-cm Path Length** (e/cm <sup>3</sup> )
Phase-Quadrature Interferometers	70.0	0.35	$6.1 \times 10^{13}$	$8 \times 10^{11} \rightarrow 3 \times 10^{13}$
	35.0	0.70	$1.5 \times 10^{13}$	$3 \times 10^{11} \rightarrow 7.5 \times 10^{12}$
Broadside Transmission-Reflection Probes	4.32	10.0	$2.3 \times 10^{11}$	
	8.6	8.0	$9.1 \times 10^{11}$	
	17.0	7.0	$3.6 \times 10^{12}$	
	35.0	6.0	$1.5 \times 10^{13}$	
	70.0	6.0	$6.1 \times 10^{13}$	
Oblique Doppler Radar	35.0	6.0		
<hr/>				
Resonant R-F Cavity	0.450	Cavity Dimensions: 6-in.-diam Entrance and Exit 12-in.-Axial Measurement Length		Range of Measurable Total Electron Population: $4 \times 10^8 \rightarrow 2 \times 10^{11}$

\*Beam width is dependent upon the particular horn-lens antenna used. Beam width can be varied by altering the effective focal length of the antenna.

\*\*Lower limits of measurable electron density correspond to a measured interferometric phase shift of 5 deg; upper limits correspond to an electron density of one-half that required to produce cutoff, over a 1-cm path length.

TABLE IV  
PHOTOMULTIPLIER RADIOMETER SPECTRAL CHARACTERISTICS

Photomultiplier Response*	Nominal Filter Center Wavelength ( $\text{\AA}$ )	Nominal Filter Bandwidth at 50% Transmission ( $\text{\AA}$ )
<u>NARROW BAND UNITS</u>		
S-5	2245	280
S-5	2485	210
S-5	2745	250
S-5	3010	320
S-5	3675	550
S-5	4330	450
S-5	5280	1015
S-10	6140	385
S-1	7760	1155
S-1	9680	1560
<u>BROAD BAND UNITS</u>		
S-5	3400	2200-5100
S-10	4500	3500-6000
S-1	8000	6100-9600

\*Alpha-numerical designations indicate spectral response characteristics adopted as standards by the Electronics Industries Association.

TABLE V  
SPECTROGRAPH CHARACTERISTICS

Type	Quantity	Aperture Ratio	Total Wavelength Capability* (First Order) (Å)	Wavelength Increment per Exposure (First Order) (Å)	Linear Reciprocal Film Plane	
					Dispersion (First Order) (Å/mm)	Resolution (Å)
Ballistic (Transmission Grating)	2	f/2.5	3750-6500	2750	100	90
3/4-m Grating	2**	f/8.3	2000-10,000	2500	20	2
3/4-m Prism	1	f/14	3750-6500	2750	25 0 (@ 5000 Å)	5 5 (@ 5000 Å)
1-m Grating	1	f/8.6	2,000-10,000	700	8	0.1

\*Spectral bandspreads shown indicate limits of the spectrographs themselves. Practical considerations (e.g., range windows) customarily reduce wavelength capability to the range 3750-6500 Å. However, the broader limits shown can be approached by exercise of special precautions.

\*\*One of these instruments is equipped with a group of six photomultipliers to enable time-resolved readout of radiant energy intensities at selected wavelengths. Of these photomultipliers, two accommodate 5-Å bandwidths, and the remaining four accommodate bandwidths of 100 Å on either side of these two 5-Å bands. Use of the photomultipliers does not interfere with the normal functioning of the spectrograph in recording spectra on film.

UNCLASSIFIED

Security Classification

DOCUMENT CONTROL DATA - R&D		
(Security classification of title, body of abstract and indexing annotation must be entered when the overall report is classified)		
1. ORIGINATING ACTIVITY (Corporate author) Arnold Engineering Development Center ARO, Inc., Operating Contractor Arnold Air Force Station, Tennessee		2a. REPORT SECURITY CLASSIFICATION UNCLASSIFIED
		2b. GROUP N/A
3. REPORT TITLE THE VON KARMAN GAS DYNAMICS FACILITY 1000-FT HYPERVELOCITY RANGE - DESCRIPTION, CAPABILITIES, AND EARLY TEST RESULTS		
4. DESCRIPTIVE NOTES (Type of report and inclusive dates) N/A		
5. AUTHOR(S) (Last name, first name, initial)  Compiled by Clemens, P. L., ARO, Inc.		
6. REPORT DATE November 1966	7a. TOTAL NO. OF PAGES 52	7b. NO. OF REFS 21
8a. CONTRACT OR GRANT NO. AF40(600)-1200	9a. ORIGINATOR'S REPORT NUMBER(S)  AEDC-TR-66-197	
b. PROJECT NO.  c.  d.	9b. OTHER REPORT NO(S) (Any other numbers that may be assigned this report) N/A	
10. AVAILABILITY/LIMITATION NOTICES This document is subject to special export controls and each transmittal to foreign governments or foreign nationals may be made only with prior approval of Arnold Engineering Development Center (AETS) Arnold AF Station, Tennessee.		
11. SUPPLEMENTARY NOTES  Available from DDC		12. SPONSORING MILITARY ACTIVITY Arnold Engineering Development Center, Air Force Systems Command, Arnold Air Force Station, Tennessee
13. ABSTRACT The von Kármán Gas Dynamics Facility (VKF) 1000-ft Hypervelocity Range facility at the Arnold Engineering Development Center is described, and its current operating capabilities are presented. A brief sampling of test results obtained during early operation of the range is presented as well. Among these are: (1) results of sphere drag measurements over the Reynolds number range $3 \text{ Re}_2 \text{ } 10^6$ ; (2) results of the measurements of flow transition locations and wake velocities behind spheres, as obtained through the use of a 35-GHz Doppler radar system; (3) results of measurements of electron densities in the wakes of spheres, as obtained using r-f cavity and microwave techniques; (4) results of the measurement of radiation from the shock caps of spheres; and (5) results of the effect of unit Reynolds number on the location of flow transition in the wakes of cones, as measured using a high sensitivity schlieren system. In each case, the data results presented are correlated with measurements made at other establishments or with data based on available theory. The correlations are shown to be generally reasonable. An appendix describes the VKF 100-ft Hypervelocity Range K, which served as a pilot facility during the development of the 1000-ft range and which continues in service.		

DD FORM 1473  
1 JAN 64

UNCLASSIFIED

Security Classification

14. KEY WORDS	LINK A		LINK B		LINK C	
	ROLE	WT	ROLE	WT	ROLE	WT
hypervelocity ranges operation test results aerodynamic test facilities sphere drag measurements electron density measurements radiation measurement Reynolds number effects						

INSTRUCTIONS

1. **ORIGINATING ACTIVITY:** Enter the name and address of the contractor, subcontractor, grantee, Department of Defense activity or other organization (*corporate author*) issuing the report.
- 2a. **REPORT SECURITY CLASSIFICATION:** Enter the overall security classification of the report. Indicate whether "Restricted Data" is included. Marking is to be in accordance with appropriate security regulations.
- 2b. **GROUP:** Automatic downgrading is specified in DoD Directive 5200.10 and Armed Forces Industrial Manual. Enter the group number. Also, when applicable, show that optional markings have been used for Group 3 and Group 4 as authorized.
3. **REPORT TITLE:** Enter the complete report title in all capital letters. Titles in all cases should be unclassified. If a meaningful title cannot be selected without classification, show title classification in all capitals in parenthesis immediately following the title.
4. **DESCRIPTIVE NOTES:** If appropriate, enter the type of report, e.g., interim, progress, summary, annual, or final. Give the inclusive dates when a specific reporting period is covered.
5. **AUTHOR(S):** Enter the name(s) of author(s) as shown on or in the report. Enter last name, first name, middle initial. If military, show rank and branch of service. The name of the principal author is an absolute minimum requirement.
6. **REPORT DATE:** Enter the date of the report as day, month, year, or month, year. If more than one date appears on the report, use date of publication.
- 7a. **TOTAL NUMBER OF PAGES:** The total page count should follow normal pagination procedures, i.e., enter the number of pages containing information.
- 7b. **NUMBER OF REFERENCES:** Enter the total number of references cited in the report.
- 8a. **CONTRACT OR GRANT NUMBER:** If appropriate, enter the applicable number of the contract or grant under which the report was written.
- 8b, 8c, & 8d. **PROJECT NUMBER:** Enter the appropriate military department identification, such as project number, subproject number, system numbers, task number, etc.
- 9a. **ORIGINATOR'S REPORT NUMBER(S):** Enter the official report number by which the document will be identified and controlled by the originating activity. This number must be unique to this report.
- 9b. **OTHER REPORT NUMBER(S):** If the report has been assigned any other report numbers (*either by the originator or by the sponsor*), also enter this number(s).
10. **AVAILABILITY/LIMITATION NOTICES:** Enter any limitations on further dissemination of the report, other than those

imposed by security classification, using **standard statements** such as:

- (1) "Qualified requesters may obtain copies of this report from DDC."
- (2) "Foreign announcement and dissemination of this report by DDC is not authorized."
- (3) "U. S. Government agencies may obtain copies of this report directly from DDC. Other qualified DDC users shall request through \_\_\_\_\_."
- (4) "U. S. military agencies may obtain copies of this report directly from DDC. Other qualified users shall request through \_\_\_\_\_."
- (5) "All distribution of this report is controlled. Qualified DDC users shall request through \_\_\_\_\_."

If the report has been furnished to the Office of Technical Services, Department of Commerce, for sale to the public, indicate this fact and enter the price, if known.

11. **SUPPLEMENTARY NOTES:** Use for additional explanatory notes.

12. **SPONSORING MILITARY ACTIVITY:** Enter the name of the departmental project office or laboratory sponsoring (*paying for*) the research and development. Include address.

13. **ABSTRACT:** Enter an abstract giving a brief and factual summary of the document indicative of the report, even though it may also appear elsewhere in the body of the technical report. If additional space is required, a continuation sheet shall be attached.

It is highly desirable that the abstract of classified reports be unclassified. Each paragraph of the abstract shall end with an indication of the military security classification of the information in the paragraph, represented as (TS), (S), (C), or (U).

There is no limitation on the length of the abstract. However, the suggested length is from 150 to 225 words.

14. **KEY WORDS:** Key words are technically meaningful terms or short phrases that characterize a report and may be used as index entries for cataloging the report. Key words must be selected so that no security classification is required. Identifiers, such as equipment model designation, trade name, military project code name, geographic location, may be used as key words but will be followed by an indication of technical context. The assignment of links, rules, and weights is optional.